Nanoparticle-based drug delivery systems for neural interfaces - a novel approach for improved biocompatibility.

Dontsios Holmkvist, Alexander

2020

Document Version:
Publisher's PDF, also known as Version of record

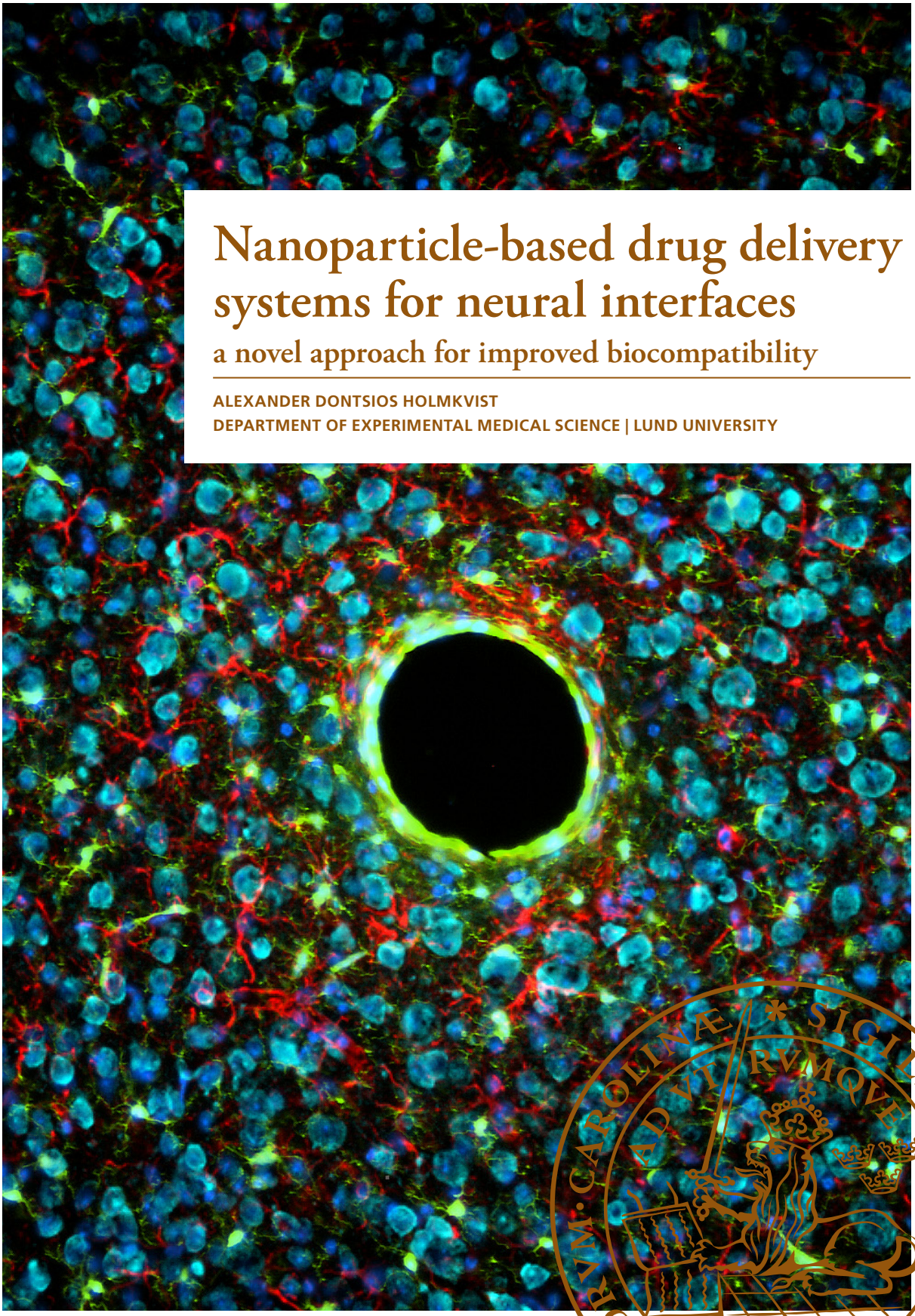

Nanoparticle-based drug delivery systems for neural interfaces

a novel approach for improved biocompatibility

ALEXANDER DONTSIOS HOLMKVIST
DEPARTMENT OF EXPERIMENTAL MEDICAL SCIENCE | LUND UNIVERSITY

Nanoparticle-based drug delivery systems for neural interfaces

Nanoparticle-based drug delivery systems for neural interfaces

a novel approach for improved biocompatibility

Alexander Dontsios Holmkvist

LUND
UNIVERSITY

DOCTORAL DISSERTATION

by due permission of the Faculty of Medicine, Lund University, Sweden.
To be defended at Medicon Village lecture hall. 19th of November 2020 at 9.00.

Faculty opponent
Professor Jöns Hilborn

Organization LUND UNIVERSITY Faculty of Medicine Department of Experimental Medical Science Neuronano Research Center Author Alexander Dontsios Holmkvist	**Document name** Doctoral dissertation **Date of issue** 2020-11-19 Sponsoring organization

Title and subtitle

Nanoparticle-based drug delivery systems for neural interfaces - a novel approach for improved biocompatibility

Abstract

The overall purpose of this thesis was to reduce brain tissue responses around implanted microelectrodes using a pharmacological strategy. One of the main aims was to develop and evaluate drug delivery systems that allow local administration of anti-inflammatory pharmaceutics. The drug Minocycline was therefore encapsulated into biodegradable poly ($_{D,L}$-lactic-*co*-glycolic acid) nanoparticles and thereby also protecting the drug from degradation. The nanoparticle construct resulted in a sustained release of Minocycline over 30 days. This constitutes a substantial increase in release time compared to what has until now been achieved for the drug. The drug-loaded nanoparticles were then embedded in a fast-dissolving gelatin coating surrounding the implant which enabled local and sustained drug release at the target site. This technique supersedes any of the conventional administration routes and minimizes the risk for systemic side effects. The developed drug delivery system was found to significantly attenuate the acute brain tissue responses around implanted microelectrodes in mice. Coatings with Minocycline-loaded nanoparticles significantly reduced the activation of microglia cells compared to control coatings with gelatin alone both 3 and 7 days post implantation. This without affecting the overall microglia population. A significant reduction of the astrocytic response was also found 7 days post implantation in comparison to control implants. No effect on neurons or total cell count was found which may suggest that the Minocycline-loaded nanoparticles are non-toxic to the central nervous system. The thesis also presents a novel nanoparticle-eluting compartmentalized microelectrode that transforms into a flexible tube once implanted.

Key words

Classification system and/or index terms (if any)

Supplementary bibliographical information	**Language:** English
ISSN and key title: 1652-8220	**ISBN:** 978-91-7619-983-1
Recipient's notes	**Number of pages** 55 / Price
	Security classification

Signature 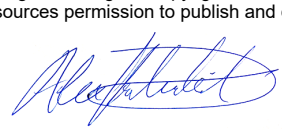 Date 2020-10-14

Nanoparticle-based drug delivery systems for neural interfaces

a novel approach for improved biocompatibility

Alexander Dontsios Holmkvist

LUND
UNIVERSITY

Cover photo by Alexander Dontsios Holmkvist 2020

Faculty of Medicine
Department of Experimental Medical Science

ISBN 978-91-7619-983-1
ISSN 1652-8220

Printed in Sweden by Media-Tryck, Lund University
Lund 2020

“It´s not who I am underneath,
but what I do that defines me”

-Batman

Table of Contents

Abbreviations

AOT	Bis(2-ethylhexyl) sulfosuccinate
BBB	Blood-brain barrier
CNS	Central Nervous System
DAPI	4′,6-diamidino-2-phenylindole dilactate
DLS	Dynamic Light Scattering
DMAB	Didodecyldimethylammonium bromide
ESD	Emulsification-solvent diffusion
FDA	Food and drug administration
GFAP	Glial fibrillary acidic protein
GFP	Green fluorescent protein
HIP	Hydrophobic ion pair
HPLC	High-performance liquid chromatography
IL	Interleukin
MC-NPs	Minocycline-loaded nanoparticles
NHS	N-hydroxysuccinimide ester
NeuN	Neuronal nuclei
NMR	Nuclear magnetic resonance
Pdi	Polydispersity index
PFA	Paraformaldehyde
PLGA	Poly($_{D,L}$-lactic-*co*-glycolic acid)
PVA	Polyvinyl alcohol
ROI	Region of interest
ROS	Reactive oxygen species
SEM	Scanning electron microscopy
TNFα	Tumor necrosis factor alpha
UV	Ultra-violet

Populärvetenskaplig sammanfattning

Hjärnan är vårt mest komplicerade organ och det svåraste att studera. Med hjälp av elektroder inopererade i hjärnan är det möjligt att elektriskt stimulera eller registrera in hjärnans elektriska aktivitet. Hjärnimplantaten ger oss därigenom möjligheten att tolka vad nervcellerna försöker åstadkomma i form av t.ex. rörelser. Elektrodimplantat har också många tillämpningar inom sjukvården. De kan t.ex. kopplas till en robotarm eller handprotes som på så sätt kan styras av en person som är förlamad. Informationen kan även användas för att förstå vissa sjukdomstillstånd i nervsystemet och hjälpa personer med olika nerv- och hjärnsjukdomar. Implantat som elektriskt stimulerar vissa områden i hjärnan används redan framgångsrikt för att lindra symptom hos patienter som drabbats av Parkinsons sjukdom.

Ett problem med permanent implanterade elektroder är dock att de orsakar en inflammation som kan skada hjärnan. Detta leder till en lokal förlust av nervceller och även bildandet av ärrvävnad runt elektroden. Den cellulära inkapslingen är elektriskt isolerande och resulterar med tiden i en förlust av den kommunikation mellan elektroden och nervcellerna man försöker uppnå.

Det övergripande syftet i denna avhandling är att minska den skadliga inflammationen i hjärnvävnaden runt elektroderna med hjälp av läkemedel. Minocyklin är ett läkemedel som skulle kunna vara lämpligt att använda i detta syfte. Läkemedlet är ett antibiotikum med antiinflammatoriska egenskaper och har använts i nästan 40 år för behandling av olika bakterieinfektioner som klamydia, svår akne och tandlossning. Mer nyligen har Minocyklin studerats för dess nervcellsskyddande effekter vid akut hjärnskada, stroke och neurodegenerativa sjukdomar. Läkemedlet måste dessvärre ges i höga doser för att få någon effekt i hjärnan. Ett av syftena i den här avhandlingen var därför att utveckla och utvärdera metoder som möjliggör lokal administrering av antiinflammatoriska läkemedel i hjärnan, dvs kunna tillföra läkemedel direkt till ett specifikt område i hjärnan. Därmed kan man undvika att ge läkemedlet via munnen eller direkt i blodet vilket även påverkar resten av kroppen.

Minocyklin kapslades därför först in i nanopartiklar som har en diameter på ca 100 nanometer (1 nanometer = 10^{-9} meter, ett hårstrå är ca 5000 nanometer i diameter) och är byggda av ett biologiskt nedbrytbart material. Partiklarna bäddades sedan in i en snabbupplösande gelatinbeläggning som omgav hjärnimplantatet. Nanopartikelkonstruktionen visade sig ge en långsam frisättning av Minocyklin under 30 dagar och gelatinbeläggning möjliggjorde en lokal frisättning av nanopartiklar med läkemedel runt hjärnimplantatet precis där det behövs. Denna teknik kompletterar de vanliga intagsvägarna för läkemedel och minimerar risken för biverkningar i resten av kroppen. De utvecklade nanopartiklarna med Minocyklin visade sig påtagligt dämpa inflammationen i hjärnvävnaden kring implanterade elektroder i möss, utan tecken på toxisk vävnadseffekt. Avhandlingen

presenterar även en ny slags elektrod som förvandlas till ett flexibelt rör efter implantation. Konstruktionen möjliggör frisläppning av nanopartiklar från en liten öppning i röret, precis där elektroden har kontakt med nervcellerna.

Sammanfattningsvis öppnar den nya nanopartikelmetoden upp helt nya möjligheter att bemästra den inflammation som vanligen uppstår runt implanterade elektroder. Detta skulle kunna vara en framtida strategi när det finns behov av permanent implantation av hjärnelektroder.

Papers included in this thesis

I. **Holmkvist AD**, Friberg A, Nilsson UJ, Schouenborg J. *Hydrophobic ion pairing of a minocycline/Ca^{2+}/AOT complex for preparation of drug-loaded PLGA nanoparticles with improved sustained release.* International Journal of Pharmaceutics. 2016; 499 (1–2): 351-357.

II. **Holmkvist AD**, Agorelius J, Forni M, Nilsson UJ, Linsmeier CE, Schouenborg J. *Local delivery of minocycline-loaded PLGA nanoparticles from gelatin-coated neural implants attenuates acute brain tissue responses in mice.* Journal of Nanobiotechnology. 2020; 18:27.

III. **Holmkvist AD**, Agorelius J, Retlund A, Nilsson UJ, Schouenborg J. *An implantable microelectrode enabling combined local release of drug loaded nanoparticles and sensing via a liquid contact.* 2020, in manuscript.

Introduction

Neural interfaces – applications and limitations

Neuro-electronic interfaces that connect the human nervous system with computers hold great potential for studying neural mechanisms and helping human patients suffering from neurodegenerative diseases. For this reason, there is a great interest in such interfaces [1]. Neuro-electronic interfaces would allow researchers to record and understand how neuronal networks process information and how this is changed by for example learning or diseases. By recording the signalling of neural networks in the brain and interpreting what the cells are trying to achieve in the form of for example movements, the electrodes can be connected to a robot arm or hand prosthesis and thus controlled by a person who is paralyzed. The interfaces may also be used for stimulation-based therapies, improving the quality of life for patients suffering from neurological injuries or disorders such as chronic pain and Parkinson's disease. However, in order to study long-term changes in information processing and also enabling treatment of neurological disorders, the foreign body response must be controlled. This response can jeopardize the functions of the implanted neuro-electronic interfaces and the physiological conditions in the adjacent tissue.

Foreign body response

The cells most commonly associated with the brain are neurons, but they only make up for less than 25% of the tissue in the brain. The remaining tissue consists of glial cells (astrocytes, microglia and oligodendrocytes) and vascular-related tissue. As an electrode is inserted into the brain, its path cuts capillaries, extracellular matrix, glial and neuronal cell processes. The mechanical trauma initiates an acute inflammatory process promoting wound closure, neuronal protection, Blood-brain barrier (BBB) repair and restriction of central nervous system (CNS) inflammation. Restoration of the damaged tissue is generally completed within a few weeks after acute uncomplicated insults. However, the reaction changes when a foreign body is left in the tissue and it develops into a chronic response instead. Over time, a coating often referred to as a "glial scar", forms around the implant that protects the intricate brain

structure from the foreign body. This glial scar is detrimental for electrode function and may adversely affect the neuronal population.

Microglia and astrocytes are assumed to be predominantly involved in the immune response in the CNS [2]. Microglia are resident macrophages of the brain responsible for clearing cellular debris and toxic substances after injury or during regular cell turnover, thereby maintaining normal cellular homeostasis. They normally reside in an inactive, highly branched state surveying the brain tissue protecting against injury and invasion. When activated, they assume a more compact morphology with phagocytic activity. Immediately after implanting an electrode, microglia begin to extend their processes towards the foreign body and damaged tissue. This fast event is demonstrated by Figure 1, an in-house *in vivo* two-photon microscopy time series of a laser induced-injury in the cortex in transgenic mice with fluorescently labelled microglial cells (B6129P-$CX_3CR\text{-}1^{GFP}$, Jackson laboratories, USA). Within 30 minutes, the processes of the nearby microglial cells reach the damaged site and appear to fuse together.

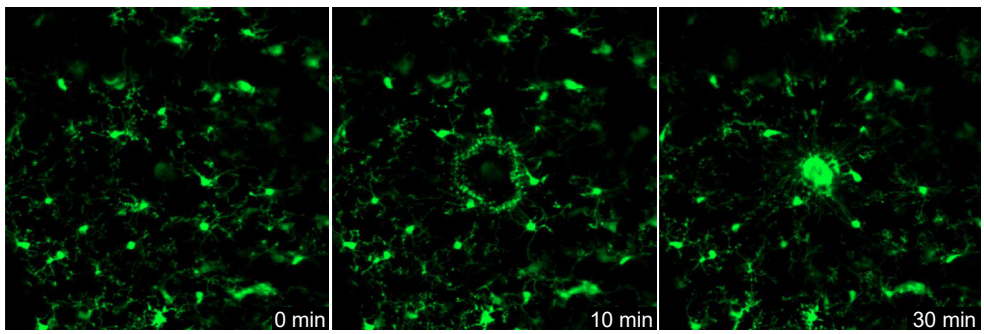

Figure 1. Time series of a laser induced injury in the cortex in $CX_3CR\text{-}1^{GFP}$ mice with fluorescently labeled microglial cells. Imaged using in-house two-photon microscopy.

Activated microglia up-regulate the production of proteolytic enzymes and pro-inflammatory cytokines including tumour necrosis factor alpha (TNFα), interleukin (IL)-1β, and IL-6 [3]. During inflammation, they also release high concentrations of reactive oxygen species (ROS) including superoxide, hydroxyl radicals, and hydrogen peroxide, all with potentially neurotoxic effects [4]. The released cytokines activate and recruit more microglial cells but also astrocytes. Astrocytes are normally responsible for supplying nerve cells with trophic support, facilitating synapse formation and function, and maintaining the composition of the extracellular fluid of the brain. Upon microglia-induced activation of astrocytes, they may lose many of their normal functions, including the ability to promote neuronal survival and tissue repair. It has also been suggested that activated astrocytes secrete a soluble toxin that rapidly kills neurons and mature oligodendrocytes, but not other CNS cell types [5].

The unusual demands of a large injury, such as implanting an electrode, may overwhelm the capacity of microglia and astrocytes. Over the following days and weeks after implantation, microglia and astrocytes migrate to the surface of the implant in an attempt to degrade the foreign object. As the electrodes are constructed to last for a long time and does not simply degrade, it causes a chronic inflammation. Instead of restoring the damaged tissue, these now reactive phenotypes of glial cells exacerbate the inflammatory response and create an unnatural environment for the neurons to function normally. Moreover, aggregated microglia and astrocytes at the surface of the implant may form an electrically insulating sheath that causes a slow dislocation of neurons away from the electrode (Fig. 2). The strength and quality of the recorded electrical signal is highly dependent on the location of the neuron relative to the electrode recording site. The maximum distance action potentials from individual neurons can be recorded at rarely exceeds 50 μm [6]. Glial encapsulation together with altered neurochemical environment will result in poor signal quality and neuronal dysfunction, both detrimental for electrode function.

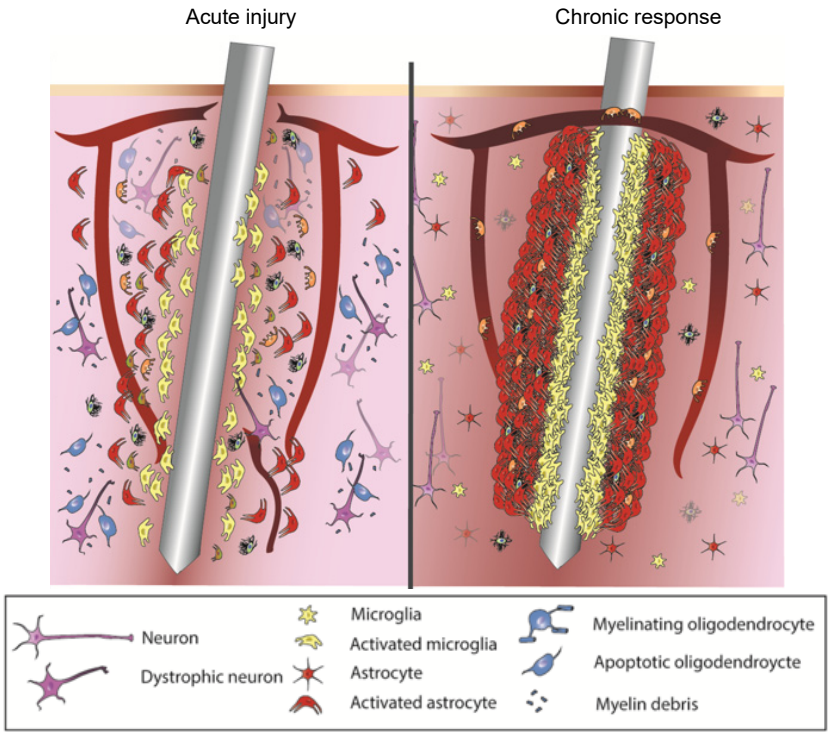

Figure 2. Illustration of the foreign body responses to implantable devices in the brain. The acute injury activate microglia and astrocytes that migrate toward the surface of the device. The chronic response may lead to the formation of a "glial scar" around the device over time. Reprinted (adapted) with permission from (Wellman SM, Kozai TDY. Understanding the Inflammatory Tissue Reaction to Brain Implants to Improve Neurochemical Sensing Performance. ACS Chemical Neuroscience. 2017;8(12):2578-82.) [7]. Copyright (2017) American Chemical Society.

Minimizing the tissue response

Electrode design

Several studies have demonstrated that electrode design and implantation technique are important factors effecting the tissue response. The brain is in constant movement relative to the skull due to arterial pulsations, respiration, and forces caused by acceleration and rotation of the body. The resulting micro-forces between anchored rigid electrodes and the brain tissue can therefore be expected to stimulate and prolong the activation of glial cells [8]. To make electrodes more biocompatible, highly flexible implants that can follow tissue movements is needed. Implantation of thin flexible electrodes requires some form of structural support to penetrate the brain without bending. Various implantation methods have therefore been developed, for example attaching the implant to a stiffer guide pin that is removed after implantation [9] or adding a hard coating that later dissolves in the brain tissue [10]. Even though these measures have shown to reduce tissue responses, the glial cell responses closest to the electrodes remain to some extent. Using anti-inflammatory pharmaceutics could be a complementary approach to further reduce the tissue reactions.

Minocycline

Antibiotic and anti-inflammatory pharmaceutics have widely been used for implantable medical devices such as prosthetic joints, pacemakers and stents. This in order to prevent implant- and surgical site infections [11, 12]. This approach could also be used for neuro-electronic devices as a complementary measure to further reduce the tissue reactions.

Minocycline is a widely used broad-spectrum antibiotic that has been in therapeutic use for almost 40 years. It belongs to the second-generation tetracyclines with improved tissue penetration, prolonged half-time and better intestinal absorption in comparison to first generation tetracyclines. The drug has most commonly been used for treatment of bacterial infections such as chlamydia, severe acne, and periodontitis [13, 14]. More recently, Minocycline has been studied for its neuroprotective effects in different animal models of acute traumatic brain injury, stroke and neurodegenerative diseases [15, 16]. It has even shown to be a promising candidate for improving the outcome of neural recordings obtained from a chronic neural interface [17]. The effects are coupled to Minocycline´s ability to inhibit activation and proliferation of microglia [18]. However, to achieve therapeutic drug concentrations in the brain by conventional administration routes, unacceptably large systemic dosages may be needed [19] which could have adverse systemic

effects [20]. To improve the therapeutic efficacy and decrease the drug dose required, local delivery from biodegradable nanoparticles could be used.

In addition to Minocycline ability to inhibit glial responses, the drug has been in therapeutic use for many years because of its antibiotic properties. Patients who undergo neurosurgery also risk bacterial infections that can cause post-neurosurgical meningitis [21]. Minocycline can therefore play a dual role, both as an anti-inflammatory agent and as an antibiotic prophylaxis, when used in this context with implantation of electrodes in the brain.

Local drug delivery systems

Approximately 98% of small molecular weight drugs and almost 100% of larger molecular weight peptides and proteins do not cross the BBB. In order to deliver therapeutics to the brain more efficiently, nanotechnology-mediated drug delivery systems are emerging. The term "nanoparticle" is a collective name for a particle of any shape with dimensions between 1 and 100 nm [22]. Drug loaded nanocarriers coated with specific compounds can significantly enhance the BBB penetration. A small enough particle coated with for example polysorbate 80 enables passive diffusion over the barrier. If the particles are coated with ligands that bind to proteins associated with the BBB instead, an active transport over the barrier is achieved and may also selectively target for example brain tumor cells [23, 24]. To eliminate the need for repeated administration, the carrier can be made of a degradable material to give a sustained release over a period of days or even weeks after administration. Poly($_{D,L}$-lactic-*co*-glycolic acid) (PLGA) is the most widely used biodegradable polymer in the CNS and undergoes hydrolysis in the body to produce the metabolite monomers, lactic acid and glycolic acid. Since the body effectively deals with these two monomers, there is minimal systemic toxicity associated by using PLGA for drug delivery or biomaterial applications [25]. Even though a nanoparticle strategy for improving BBB permeability offer more effective and non-invasive ways of delivering pharmaceutics to the brain, there is still a lack of specificity to target the area surrounding an implanted electrode. A more straight-forward strategy in this sense would be to deliver the drug-loaded nanoparticles directly from the implant.

Delivering drug-loaded nanoparticles locally from implants has been achieved by using different nanoparticle- and coating-materials. Kim et al. [26] for example, used an alginate hydrogel to deliver PLGA particles loaded with the anti-inflammatory agent Dexamethasone. Even though their study showed no significant change in impedance with time *in vivo*, alginate hydrogels are non-biodegradable in mammalian brains [27]. The coating may thereby create a long-lasting barrier between the implanted electrode and surrounding tissue, hindering neurons getting close enough to the implant for high quality recordings. Mercanzini et al. [28] used

a poly(ethylene oxide) coating with embedded poly(propylene sulfide) Dexamethasone-eluting nanoparticles. Their study showed reduced tissue reaction to the implanted microelectrode and that the coating dissolves after implantation. However, the method used for embedding the nanoparticles into the coating involved harsh processing parameters, such as high temperatures, which may be harmful for sensitive molecules. Minocycline for example, degrades easily under exposure to light, high temperatures or low and high pH [29]. In this thesis, gelatin is evaluated as the nanoparticle-carrying coating material. Gelatin is a protein material derived from natural collagen that easily breaks down into amino acids in the body. The material itself has shown beneficial effects for restoration of the BBB after acute brain injury [30] and enables mechanical support for implanting highly flexible electrodes [31].

Therefore, a nanoparticle-based drug delivery system for neural implants should be designed with regard to the following key aspects, i) the drug-loaded nanoparticles should give a sustained release of the drug that matches the inflammatory response, ii) the particles should be large enough to not diffuse freely in the brain but remain close to the implantation site where the highest concentration of the drug is needed, iii) the implant coating should preferably not affect the device function and iv) processing parameters during preparation of both coating and particles needs to be mild enough to protect the drug from degradation.

Aims

The overall purpose of this thesis was to reduce brain tissue responses around implanted microelectrodes using a pharmacological strategy. The main aim was to develop and evaluate nanoparticle-based drug delivery systems, suitable for implantable neural devices, that allow local administration of anti-inflammatory pharmaceutics.

The specific goals were:

1) To develop and characterize Minocycline loaded PLGA nanoparticles, aiming for particle sizes around 100 nm with sustained drug release over 30 days *in vitro*.
2) To develop a method for embedding minocycline-loaded PLGA nanoparticles into gelatin-coatings on neural implants.
3) To clarify *in vivo* whether the addition of these nanoparticles could reduce the acute brain tissue responses after implantation in mice.
4) To develop and characterize a novel nanoparticle-eluting microelectrode *in vitro*.

Methods and method development

This thesis has been a truly interdisciplinary research project that spans organic synthesis, analytical chemistry, surface and colloidal chemistry, drug formulation, neuro-electronic interfaces, small animal surgery, cell biology, immuno-fluorescence staining methods and foreign body responses in the brain. A general description of the methods and techniques used followed by a short discussion of key aspects and motivation within each area is given below. For detailed descriptions of the methods, the reader is referred to the articles this thesis is based on. The roman numbering refers to the different articles included in this thesis.

Preparation of nanoparticles (I, II, III)

Nanoparticles were prepared using a single oil-in-water (o/w) emulsification method often referred to as the emulsification-solvent diffusion (ESD) technique, schematically described in Figure 3. In brief, an o/w emulsion is first made from a partially water-soluble solvent containing both the biodegradable carrier-material and drug, and an aqueous solution containing a surfactant. Water is subsequently added to the two-phase system which causes diffusion of the solvent into the external water phase. This causes the polymer to precipitate in the form of nanospheres with the drug entrapped throughout the particle matrix. The organic solvent is finally evaporated resulting in a colloidal suspension stabilized by the surfactant. All prepared suspensions were lyophilized and stored in a freezer until used. Mannitol and Pluronic F-127 were added as cryoprotectants before freeze-drying to enable redispersion and prevent particle aggregation.

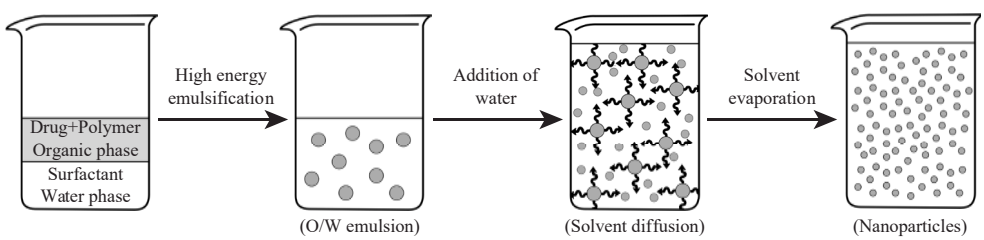

Figure 3. Schematic representation of PLGA nanoparticle preparation by the emulsificaton-solvent diffusion technique. Reprinted (adapted) with permission from Paper I.

The choice of using the ESD technique for the preparation of nanoparticles in this thesis was based on the method's compatibility with a wide range of pharmaceutics and its simplicity compared to other existing methods. The method does not require advanced equipment, such as high-pressure homogenizers [32], and can be done with standard laboratory equipment such as an ultrasonic water bath and a magnetic stirrer. It is also known to provide high reproducibility. The resulting nanosphere composition is a homogenous particle with the drug entrapped throughout the particle matrix. This type of particle generally generate longer and more stable release times compared to liposomes or nanocapsules (a solid shell structure that surrounds a core-forming space) prepared by double emulsion techniques [33].

Poly($_{D,L}$-lactic-*co*-glycolic acid) (PLGA), an FDA-approved biodegradable polymer, was chosen as the particulate carrier-material due to its history of safe use in the CNS [34]. PLGA degrades by hydrolysis of its ester linkages in aqueous environments to lactic and glycolic acid which are finally eliminated from the body as carbon dioxide and water. As the polymer degrades and erodes, the drug release kinetics is a function of polymer degradation as well as drug diffusion through polymer matrix. PLGA also enables the possibility to tune the release rate by choosing the composition or ratio between the lactic and glycolic acid monomer. Glycolic acid is slightly more hydrophilic than lactic acid, leading to increased hydrolysis rates and therefore faster release rates with increased glycolic acid content.

Didodecyldimethylammonium bromide (DMAB), a double-chained cationic quaternary ammonium surfactant, was chosen as the stabilizing agent due to reports of generating smaller sized nanoparticles compared the more commonly used stabilizer polyvinyl alcohol (PVA) [35]. DMAB also generate particles with cationic surface charge which could increase the rate and extent of their internalization caused from ionic interactions with the negatively charged cell membrane [25]. Different DMAB concentrations were evaluated as a means of adjusting the particle size, aiming for 100 nm.

Hydrophobic ion pairing (I, II)

Encapsulating pharmaceutics by the ESD method requires that the drug stays in the oil phase during the preparation and is thus more suitable for lipophilic substances. The initial project plan included screening of suitable immunomodulating drugs, of which many are lipophilic [36, 37], this is the reason why the ESD method was selected. Minocycline is often referred to in the literature as the most lipophilic drugs within the tetracycline family [38], but from a drug formulating perspective it is highly water soluble. In order to encapsulate Minocycline by the ESD technique, the solubility of the drug was altered by the concepts of hydrophobic ion pairing. This involves replacement of the polar counter ions with an ionic detergent. Furthermore, Minocycline is known to be unstable and degrades under e.g. exposure

to light, which could lead to degradation of the drug during the preparation process. Advantageously, Minocycline can be stabilized and interacts strongly with calcium ions (Ca^{2+}) [39]. Therefore, a hydrophobic ion pair complex of minocycline, Ca^{2+} and the anionic surfactant bis(2-ethylhexyl) sulfosuccinate (AOT) was developed (Fig. 4).

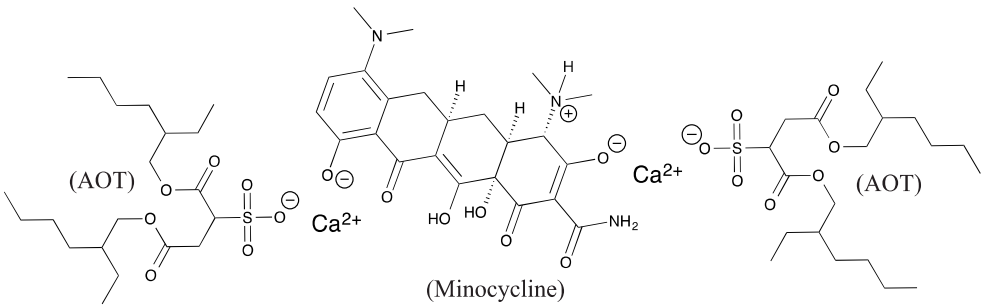

Figure 4. Hydrophobic ion pair complex of minocycline, Ca^{2+} ions and the ionic detergent bis(2-ethylhexyl) sulfosuccinate AOT. Reprinted (adapted) with permission from Paper I.

The formation of the hydrophobic ion pair complex was verified using nuclear magnetic resonance spectroscopy (NMR). The Minocycline/Ca^{2+}/AOT-complex and control samples of Minocycline, Minocycline/Ca^{2+}, AOT, and Minocycline/AOT were dissolved in deuterated chloroform. ^{1}H NMR spectra of each individual sample was recorded on a Bruker Avance II 400MHz spectrometer. The recorded spectra strongly suggested that a Minocycline/Ca^{2+}/AOT-complex was formed and that no interaction occurs between Minocycline and AOT in the absence of Ca^{2+} ions.

Fluorescently labelled nanoparticles (II, III)

Fluorescently labelled nanoparticles were prepared in order to visualize the particles during the development of the gelatin coating and the tubular microelectrode. A fluorescent dye was covalently attached to the PLGA chain [40]. The carboxylic group of PLGA was first activated through the formation of N-succinimide ester (NHS) (Scheme 1). After the reaction, the precipitated biproduct dicyclohexylurea (not shown in scheme) was removed by filtration. The activated polymer was then conjugated with Alexa Fluor 568 cadaverine through an amide bond between the NHS-activated end group of the polymer and the amine group on the fluorescent dye (Scheme 2). Drug-free fluorescently labelled nanoparticles were then prepared according to the particle preparation method described above using fluorescently labelled PLGA mixed with non-labelled PLGA in the ratio of 1:3 (w:w).

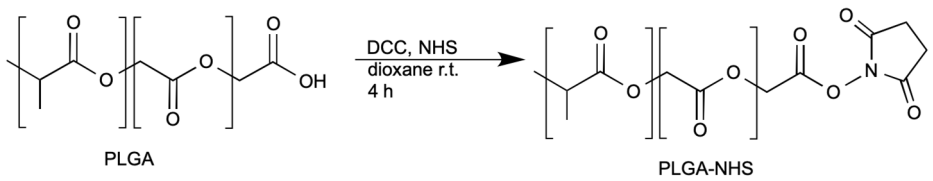

Scheme 1. N-hydroxysuccinimide (NHS) activation of the carbocylic endgroup of the PLGA-chain through the reaction with dicyclohexylcarbodiimide (DCC) in anhydrous dioxane.

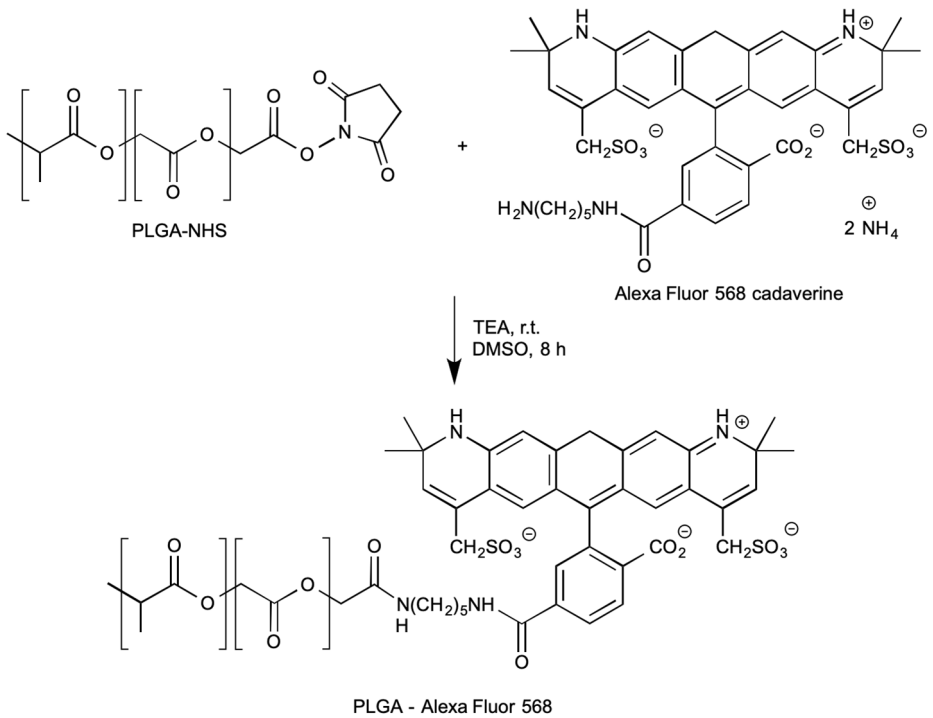

Scheme 2. Conjugation of NHS-activated PLGA with the fluorescent dye Alexa Fluor 568 in dimethyl sulfoxide (DMSO) with excess amounts of triethylamine (TEA).

Characterization of nanoparticles

Particles size and morphology

Dynamic light scattering (DLS) was used for measuring the size, polydispersity index (pdi) and zeta potential of the prepared nanoparticles. This method offers fast analysis and requires minimal sample preparation. The method was therefore ideal for comparing different nanoparticle formulations during the developmental work. Particles suspended in liquid undergo Brownian motion, and the method measures

the random changes in the intensity of light scattered from a suspension. The fluctuation in scattering intensity is then converted to particle size through the Stokes-Einstein equation [41]. The instrument therefore reports the size of a hypothetical hard sphere that diffuses in the same fashion as the particle being measured. In order to validate DLS as an appropriate measuring method for our particles, the shape of the nanoparticles was investigated by scanning electron microscopy (SEM).

Drug loading and in-vitro release (I)

The amount of Minocycline entrapped in the nanoparticles was quantified using high-performance liquid chromatography (HPLC) with ultra-violet (UV) detection. The *in vitro* drug release was studied in artificial cerebrospinal fluid using a dialysis method and quantified by HPLC-UV.

Gelatin coating and nanoparticle embedding (II)

Stainless steel needles were used as a model for neural implants. In brief, the needles were first insulated with Parylene-C, dipped in warm gelatin and allowed to dry to create the gelatin coating. The coated needles were then immersed in a nanoparticle suspension at room temperature, allowing the gelatin coating to swell and absorb the suspension without dissolving. The thickness of the coating was measured before and after nanoparticle embedding. The release of fluorescently labelled nanoparticles from coated needles were studied *in vitro* in agarose gel, a medium widely considered to be a viable model of the brain [42].

Development of the dip-coating method included numerous initial studies on the gelatin solution, including evaluation of different concentrations, temperatures and dipping speed. The absorption of nanoparticles was initially developed by using a casted gelatin rod that was immersed in a suspension of fluorescent nanoparticles in order to visualize how far and fast the nanoparticles were absorbed. A small section of the gelatin rod was then cut and placed between two cover glasses and the cross section was imaged using confocal microscopy (Zeiss LSM 510 with an Acroplan 40×/0.8W objective). Two laser lines, 488 nm and 543 nm were used for sequential excitation of gelatin and the fluorescent nanoparticles, respectively. Figure 5 shows the cross section of a dry gelatin rod after absorption of a nanoparticle suspension with the immersion time of two minutes.

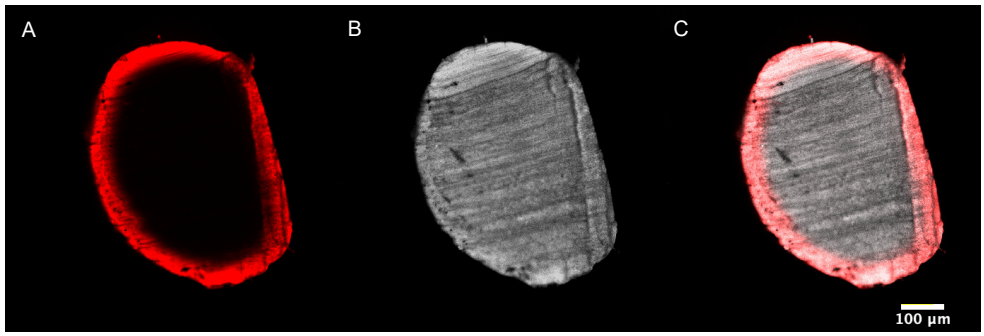

Figure 5. Confocal image of fluorescently labelled nanoparticles (A) absorbed in a gelatin rod (B). (C) is the merged image of (A) and (B).

However, when absorbing particles into gelatin on the coated needles using the same immersion time, the gelatin coatings became deformed after drying. This led to the suspicion that the immersion time was too long for the needles with considerably thinner gelatin coating, causing the gelatin to detach (but not dissolve) from the needle and then dry in a deformed conformation. To find the optimal immersion time, the swelling behavior of gelatin when on needles was therefore studied using light microscopy. Figure 6 shows a time series of a gelatin coated needle after addition of an aqueous solution containing cryoprotectants. The swelling study showed that the coating swelled approximately ten times its original size already after 20 seconds and did not swell substantially more until the coating started to detach from the needle after 45 seconds. The immersion time was therefore set to 30 seconds for absorbing of the nanoparticle suspension.

The amount of nanoparticles absorbed in the coating was estimated from the following assumptions: i) the nanoparticles diffuse unhindered into the gelatin coating during swelling and ii) the swelled gelatin coating contained the same concentration of nanoparticles as the surrounding suspension the implant was immersed in.

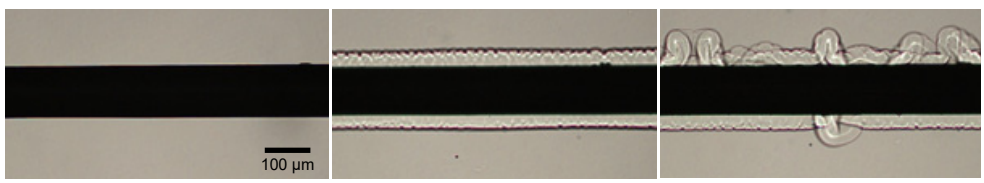

Figure 6. Time series for the swelling of a gelatin coating on a needle. The coating has swelled approximately 10 times its original size after 30 seconds and has started to deform and detach from the needle after 60 seconds.

Surgery and implantation (II)

Approval for the animal experiments was obtained in advance from the Malmö/Lund Animal Ethics Committee on Animal Experiments (ethical permit M61-13) and all experiments in this work conform to the regulatory standards of this approval.

Transgenic mice (both male and female) that express green fluorescent protein ($CX_3CR\text{-}1^{GFP}$) in brain microglia were used for the *in vivo* study on brain tissue responses to implanted needles. The mice were anaesthetized with isoflurane, shaved, and given subcutaneous injection of local analgesia. Small craniotomies (1 mm diameter) were carefully drilled midways between bregma and lambda, around 1 mm laterally of the midline. The coated needles were cut to 3 mm and placed inside a glass capillary filled with paraffin oil to avoid water uptake and swelling of gelatin before entering the cortex. Bilateral implantations of a gelatin-coated needle (control) and a gelatin-coated needle with embedded Minocycline-loaded nanoparticles were done in each mouse. The needles were implanted using a hydraulic micropositioner at the speed of 500 μm/s to a depth of 3 mm below cortical surface.

Histology (II)

The brain tissue responses to the implanted needles were evaluated at 3 or 7 days after implantation. In brief, the mice were deeply anaesthetized by an intraperitoneal injection of pentobarbital and transcardially perfused with saline and paraformaldehyde (PFA). The brains were subsequently removed and post-fixated in PFA overnight. Needles were explanted before the brains were horizontally sectioned (16 μm) on a cryostat.

Immunohistochemistry

Two sections from a depth of approximately 400–500 μm into the cortex at each implantation site were then stained using the following primary antibodies: rabbit anti-CD68 to identify activated microglia, rabbit anti-NeuN to identify neurons and chicken anti-GFAP to identify astrocytes. All tissue sections were also stained with 4′,6-diamidino-2-phenylindole dilactate (DAPI) to visualize cell nuclei. As already mentioned, the transgenic mice express green fluorescent protein (GFP) for all brain microglia (that is both resting and activated), characterized by high expression of the chemokine receptor $CX_3CR\text{-}1$. Secondary antibodies conjugated to Alexa Fluor 647 and Alexa Fluor 594 were therefore used to enable differentiation of four colors in each section.

Image acquisition and analysis

The stained sections were imaged using fluorescence microscopy. Regions of interest (ROIs) were set to 0–50 µm and 50–100 µm from the border of the implantation site. The response for all microglia ($CX_3CR\text{-}1^{GFP}$), activated microglia (CD68) and astrocytes (glial fibrillary acidic protein (GFAP)) was quantified by measuring the proportion of stained area within each ROI. The number of neurons (neuronal nuclei (NeuN) (with a DAPI-positive nucleus as an inclusion criteria) and all cell nuclei (DAPI) were manually counted within each ROI.

Mann–Whitney test was used to compare the experimental groups within each ROI and time point, p-values < 0.05 were considered significant.

Development of the tubular microelectrode (III)

The nanoparticle eluting microelectrode was developed from an already existing electrode construction developed in our laboratory. The original microelectrode consisted of a gold wire coated with an electrospun layer of glucose and an insulating Parylene-C coating. The probe has a hole opening in the distal part, allowing fluidic connection with the surrounding tissue. The structure provides sufficient mechanical strength during insertion into the brain but transforms into a flexible tube once implanted.

To embed the nanoparticles into the compartmentalized construction, four potential designs (illustrated in Fig. 7) were initially considered and evaluated with regard to electrode function and manufacturing process. All designs comprised a gold wire as the core registering lead and an insulating Parylene-C coating as the outer layer. The designs were the following: A) a glucose compartment with embedded nanoparticles, applied by electrospinning of a glucose solution with suspended nanoparticles. B) electrophoretic deposition of the nanoparticles directly onto the gold lead (inspired by stent technology [43] and making use of the nanoparticles' positive surface charge) and an outer electrospun compartment of glucose. C) a gelatin compartment with embedded nanoparticles. D) an inner compartment of gelatin with embedded nanoparticles and an outer compartment of electrospun glucose.

Characterisation of the tubular electrodes was done using SEM imaging, impedance measurements and fluorescent microscopy. The *in vitro* release of fluorescent nanoparticles was studied in agarose at 37 °C.

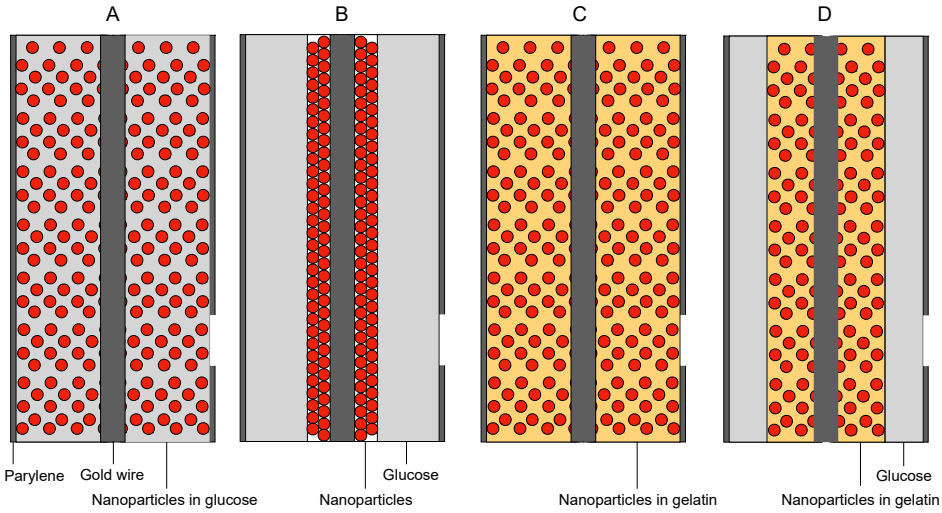

Figure 7. Tubular electrode designs containing nanoaparticles. All designs comprised a gold wire as the core registrating lead and an insulating Parylene-C coating as the outer layer. A) A glucose compartment with embedded nanoparticles. B) Nanoparticles deposited directly of the onto the gold lead with an outer glucose compartment. C) A gelatin compartment with embedded nanoparticles. D) An inner compartment of gelatin with embedded nanoparticles and an outer compartment of glucose.

Results and comments

1) Minocycline loaded PLGA nanoparticles, *in vitro* (I)

The first aim in this thesis was to develop and characterize Minocycline-loaded PLGA nanoparticles with sizes around 100 nm and an *in vitro* drug release over at least 30 days. The size of the particles was chosen based on the idea that the particles would remain relatively stationary and not diffuse freely in the brain extracellular space once deposited. The ‘‘pore size’’ of the extracellular space is considered to be ~40 nm [44, 45]. The released drug would thereby be concentrated to the region near the implants where it is most needed. The drug release duration was chosen to match the progression of the brain tissue responses after injury [46]. It has been suggested that Minocycline should be administered at high doses initially for 7 days to attenuate the acute inflammatory response, followed by a lower dose for 3-6 weeks to attenuate the chronic response [47].

Development of the particles started with preparation of drug-free PLGA nanoparticles using the emulsification-solvent diffusion (ESD) technique. Formulations with different concentrations of the surfactant DMAB were evaluated and finally set to 0.10% which resulted in 150 nm sized monodisperse nanoparticles with a positive zeta potential. Lower concentrations resulted in unsuccessful emulsions or larger particles with broader size distributions and negative zeta potentials. Figure 8A shows the size distribution curves generated from dynamic light scattering (DLS) measurements of blank and drug-loaded nanoparticles.

The DLS method measures the random intensity changes of light scattered from a suspension. The fluctuation in scattering intensity is then used to calculate the size, poly dispersity index (pdi) and zeta potential of particles within the sample. The zeta potential gives information on how well the particles tend to repel each other and thereby withstand aggregation. Particles with zeta potentials over +30 mV or less than -30 mV will form stable colloidal suspensions. The pdi is a dimensionless measure of the broadness of the size distribution and ranges between 0 and 1. A dispersion may be considered monodisperse (pdi < 0.1) if 90% of the distribution lies within ±5% of the average size.

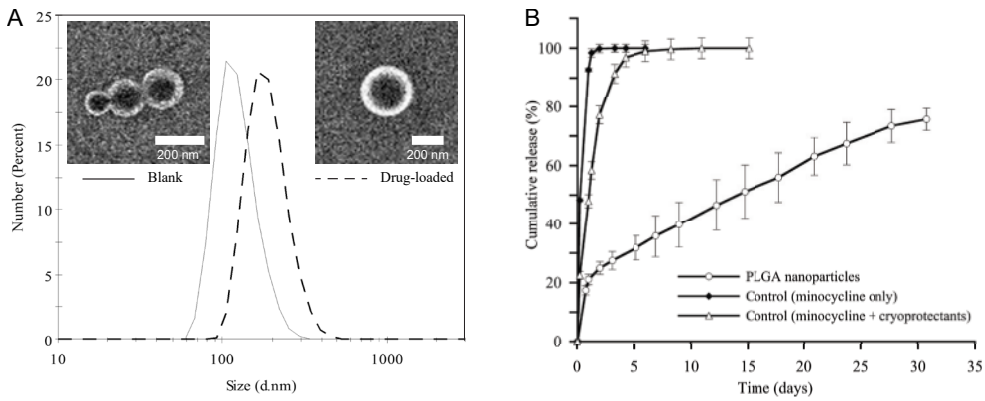

Figure 8. A) DLS size distribution curves and SEM micrographs of blank and Minocycline-loaded PLGA nanoparticles. B) *In vitro* release in artificial cerebrospinal fluid from minocycline loaded PLGA nanoparticles and control curves of minocycline only and minocycline together with cryoprotectants. Reprinted (adapted) with permission from Paper I.

The DLS method reports the size of a hypothetical hard sphere that diffuses in the same fashion as that of the particle being measured. In order to validate the size results obtained with DLS, the shape of the nanoparticles was also investigated by SEM imaging. The SEM micrographs (Fig. 8A) confirm that both the drug-free and drug-loaded nanoparticles were spherical and therefore it was concluded that DLS was an appropriate method to use for characterizing the prepared nanoparticle suspensions.

The second step was to encapsulate Minocycline using the ESD technique, a preparation method generally more suitable for encapsulation of lipophilic substances. A novel hydrophobic ion pair (HIP) of Minocycline, Ca^{2+} and the anionic surfactant bis(2-ethylhexyl) sulfosuccinate (AOT) was developed which enabled encapsulation of the hydrophilic drug using the ESD technique. The formation of the HIP-complex was verified using nuclear magnetic resonance spectroscopy (NMR). The ^{1}H NMR spectra of the HIP-complex and control samples are shown in Figure 9. Preparation of nanoparticles with the encapsulated drug-complex resulted in particle sizes around 220 nm, a drug content of 1.12%, and an entrapment efficiency of 43%. The formulation showed a sustained drug release *in vitro* over 30 days in artificial cerebrospinal fluid (Fig. 8B).

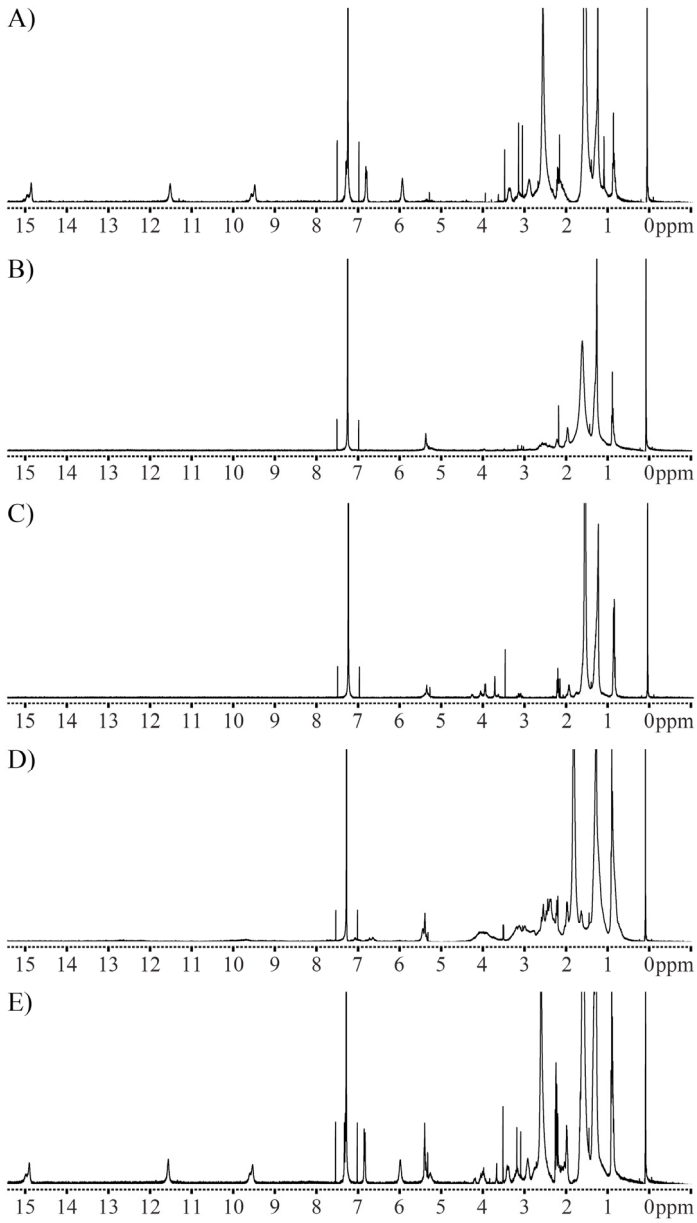

Figure 9. ^{1}H NMR spectra of (A) Minocycline (MC); (B) MC/Ca^{2+}; (C) AOT; (D) MC/Ca^{2+}/AOT; (E) MC/AOT. Comparison of spectra (A) and (B) show changes in intensity and shape for minocycline's characteristic peaks at 5.95, 6.83, 7.31, 9.50, 11.53 and 14.87 ppm, which indicates minocycline complexation with Ca^{2+} ions. Comparison of spectra (C) and (D) show a broadening of AOT's characteristic peaks at 3.74– 3.98 ppm in the presence of the Minocycline/Ca^{2+} chelate, strongly suggesting that a Minocycline/Ca^{2+}/AOT-complex has formed. Spectrum (E) of AOT and Minocycline in the absences of Ca^{2+} appears as a combination of spectra (A) and (C), indicating no interaction occurs between Minocycline and AOT in the absence of Ca^{2+}. Reprinted (adapted) with permission from Paper I.

2) Gelatin coating and nanoparticle embedding (II)

The second aim in this thesis was to develop a method for embedding the nanoparticles into gelatin-coatings on neural implants. In order to visualize the particles during the development work (Paper II and III), a fluorescent dye (Alexa Fluor 568) was covalently attached to the PLGA chain before preparing nanoparticles. DLS measurements showed that the fluorescently labelled nanoparticles had similar size, polydispersity index (pdi) and zeta potential as of the nanoparticles prepared in Paper I. The different nanoparticle formulations and characteristics are summarized in Table 1. The similar characteristics between the formulations suggest that the fluorescent dye did not interfere with the formation of nanoparticles and that the fluorescent nanoparticles were a useful surrogate for drug-loaded nanoparticles during the development work.

Table 1
Summary of Size, PDI and zeta potential of the prepared nanoparticles used in this thesis (mean ± s.d., n = 3).

Nanoparticle formulation	Size (d. nm)	PDI	Zeta pot. (mV)
Drug free	150 ± 10	0.06 ± 0.020	+57 ±7
Minocycline-loaded	220 ± 6	0.07 ± 0.004	+55 ± 4
Fluorescently labelled	150 ± 2	0.07 ± 0.010	+62 ± 3

An absorption method was developed to embed the nanoparticles into the gelatin coating. Mixing the particles directly into gelatin would have been easier, but as the gelatin solution needs to be heated at 50 °C during the dip-coating step, there would be a risk of melting the particles, degrading the drug and/or causing the drug to be released. The absorption method developed permitted the nanoparticle suspensions to be embedded into the gelatin coating at room temperature. The method also allowed minimal consumption of the laboriously prepared nanoparticle suspension.

The final gelatin coatings with embedded nanoparticles had a dry thickness of 9.1 ± 1.2 μm (mean ± standard deviation, n = 7). This thickness was almost doubled compared to the initial gelatin coating alone (4.8 ± 0.9 μm). The amounts of nanoparticles absorbed in the coating was estimated to a total amount of 1 μg nanoparticles on a 3 mm part of the implant. This would correspond to a Minocycline content of 34 ng. Figure 10A shows a needle with fluorescently labelled nanoparticles embedded in the gelatin coating. Figure 10B shows a time series of the *in vitro* release study in agarose gel and it was concluded that the gelatin coating would stay intact during implantation and that the nanoparticles spread radially ~850 μm from the implant over 10 minutes.

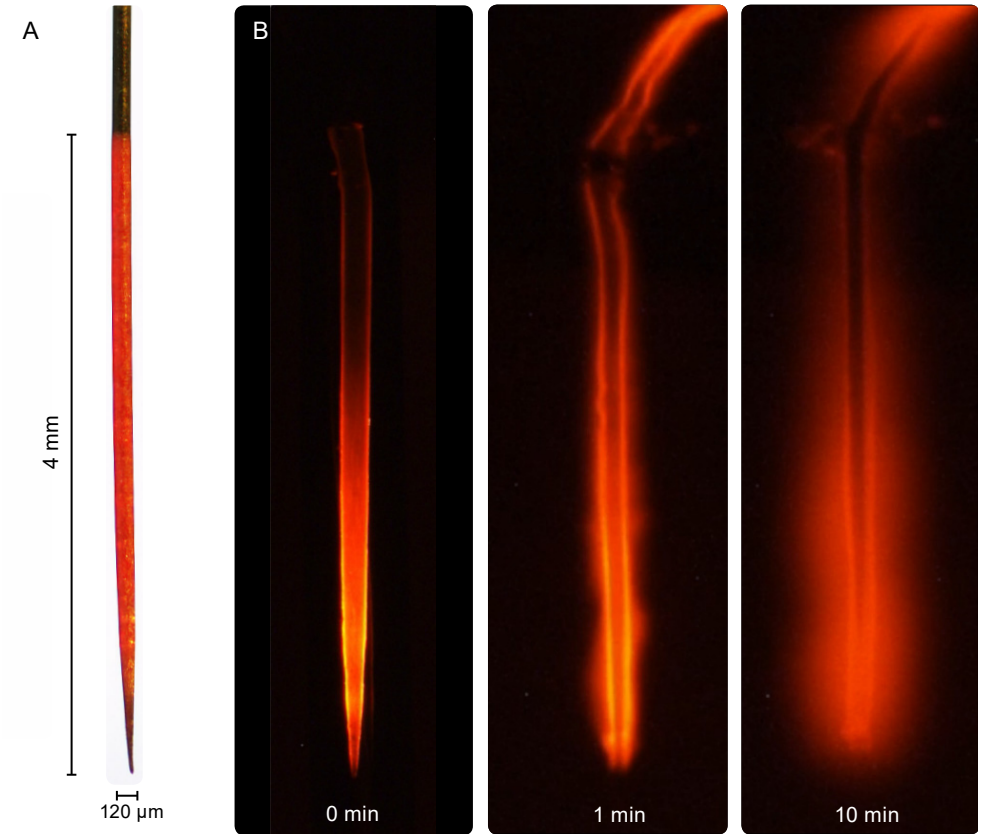

Figure 10. A) A stainless steel needle coated with gelatin and fluorescent nanoparticles. B) Time series of the *in vitro* release of nanoparticles in agarose gel. Reprinted (adapted) with permission from Paper II.

3) *In vivo* effects on brain tissue responses (II)

The third aim of this thesis was to clarify *in vivo* whether the addition of Minocycline-loaded nanoparticles could reduce the acute brain tissue responses after implantation in mice. A study with bilaterally implanted free-floating needles was used as a model for brain implants. The implanted needles had either been coated with gelatin only (control) or gelatin and embedded Minocycline-loaded nanoparticles (MC-NP). The tissue response was quantified in an inner (0–50 µm from border of implant) and an outer (50–100 µm) region of interest (ROI) surrounding the implantation site. Figure 11 and 12 shows representative immunofluorescent images of the brain tissue responses around implantation sites at 3 and 7 days after implantation.

Reduced microglia activation

Coatings with MC-NPs was shown to significantly reduce the activation of microglia cells (CD68) both 3 and 7 days after implantation compared to the control implants (Fig. 11A-D). After 3 days, the reduction was significant in both inner ($p = 0.0079$) and outer ($p = 0.0052$) ROIs. The response had almost disappeared in both groups after 7 days (Fig. 11C, D), but was still significant around implants with MC-NPs compared to the control implants in the inner ROI ($p = 0.0289$). The overall microglia population ($CX_3CR\text{-}1^{GFP}$) (Fig 11E-H), however, showed no significant difference between the groups at either time point. These observations suggest that the MC-NPs selectively attenuates the activation of microglial cells without effecting the overall population of microglia.

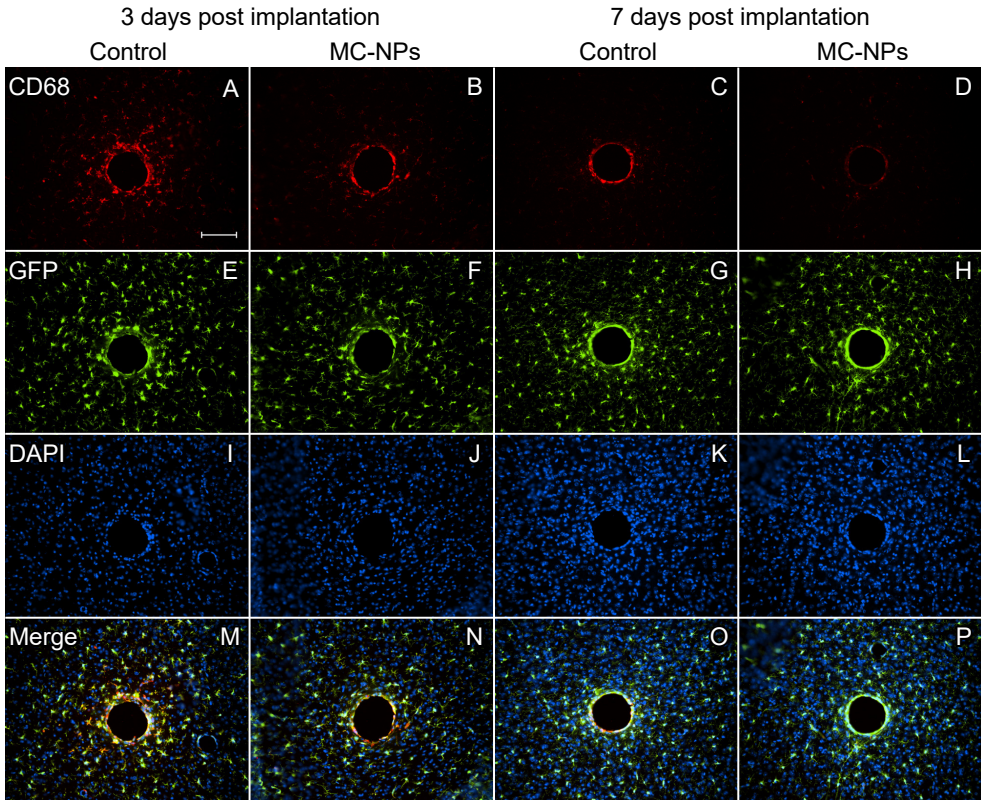

Figure 11. Representative immunofluorescent images of the microglial response. Tissue surrounding gelatin-coated needles with or without embedded MC-NPs at 3 days (two left columns) and 7 days (two right columns) post implantation. Images show activated microglia (CD68) (A–D), $CX_3CR\text{-}1^{GFP}$ positive microglia (GFP) (E–H), cell nuclei (DAPI) (I–L), and merge (M–P). Scale bar = 100 µm. Reprinted (adapted) with permission from Paper II.

Reduced astrocytic response

Both control and MC-NPs implants showed an overall increase in the astrocytic response after 7 days compared to 3 days (Fig. 12A-D). Implants with MC-NPs however, was shown to significantly reduce the astrocytic response in the inner ROI ($p = 0.0401$) at 7 days compared to the control. It remains to be determined, if this delayed reduction is a direct effect from Minocycline or a secondary effect from the decreased microglia activation at earlier time points.

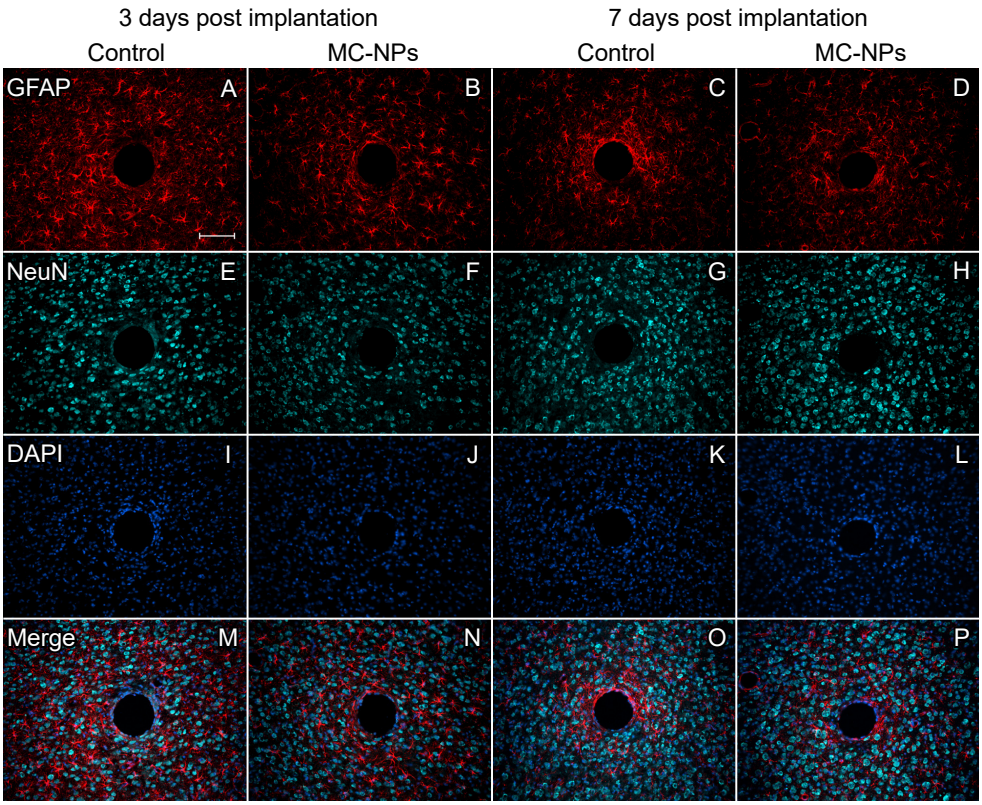

Figure 12. Representative immunofluorescent images of the astrocytic and neuronal response. Tissue surrounding gelatin-coated needles with or without embedded MC-NPs at 3 days (two left columns) and 7 days (two right columns) post implantation. Images show astrocytes (GFAP) (A–D), neurons (NeuN) (E–H), cell nuclei (DAPI) (I–L), and merge (M–P). Scale bar = 100 µm. Reprinted (adapted) with permission from Paper II.

Neuroprotection

Reduction of both activated microglia and reactive astrocytes should be beneficial for neuronal survival as these are known to release components with neurotoxic effects. In this study, we found no difference in neuronal density between the groups at either time point (Fig. 12E-H). This may be due to the gelatin coating itself [48,

49] and the study design using free floating implants [50], both of which are beneficial for neuronal survival. Furthermore, there was no significant differences found between groups for all cell nuclei at either time point (Fig. 11I-L and 12I–L).

Altogether, the combined findings point to the conclusion that neither the number of neurons, overall microglia population nor the total number of cells are changed by the nanoparticles during the 7-day period. This may suggest that the MC-NPs are non-toxic.

4) Development of a tubular microelectrode (III)

The last aim in this thesis was to develop and characterize a novel nanoparticle-eluting microelectrode *in vitro*. The four hypothetical designs presented in Figure 7 were evaluated with regard to electrode function and manufacturing process. Design D was found to be the only construction that met the criteria of not affecting electrode function and had a mild enough manufacturing process that did not compromise the integrity of the embedded nanoparticles or drug load. A short comment on each design is given below.

Design A was never evaluated due to a risk of compromising the integrity of the nanoparticles and drug during the electrospinning process. The process would use a glucose solution in ethanol and water with suspended nanoparticles which then would be electrospun onto the gold wire. The electrospinning method developed in our laboratory requires high temperature (45-50 °C) for 40 minutes plus additional preheating time. PLGA with a glass transition temperature of 40-45 °C [51] would most likely be affected by the high temperature and might cause the nanoparticles to aggregate and/or release their drug load into the solution [33]. Hence, the strategy of using nanoparticles as a means of sustained release would be lost/compromised and it would also risk that Minocycline would degrade as it is known to be even less stable in solution than a dry powder [39, 52].

Design B was prepared by dragging a gold wire (attached on a frame) through a drop of nanoparticle suspension. Direct current was applied over the syringe needle (cathode) and the wire (anode) and then characterized using fluorescence microscopy. Control experiment using the same setup without current were also made. Preliminary results showed that the nanoparticles were deposited in greater extent when direct current was applied. The full development of this technique was however not completed as characterization or estimation of the deposited amounts of nanoparticles and drug would be challenging and time consuming.

Design C was prepared by dip coating the gold wire in gelatin, insulating it with Parylene-C and making a hole opening. Studies on the coating's integrity was done by immersing the tubes in saline. SEM images (Fig. 13A, B) revealed that the

insulation and hole opening of these tubes were compromised due to forces created by the swelling of the gelatin compartment when it absorbs water.

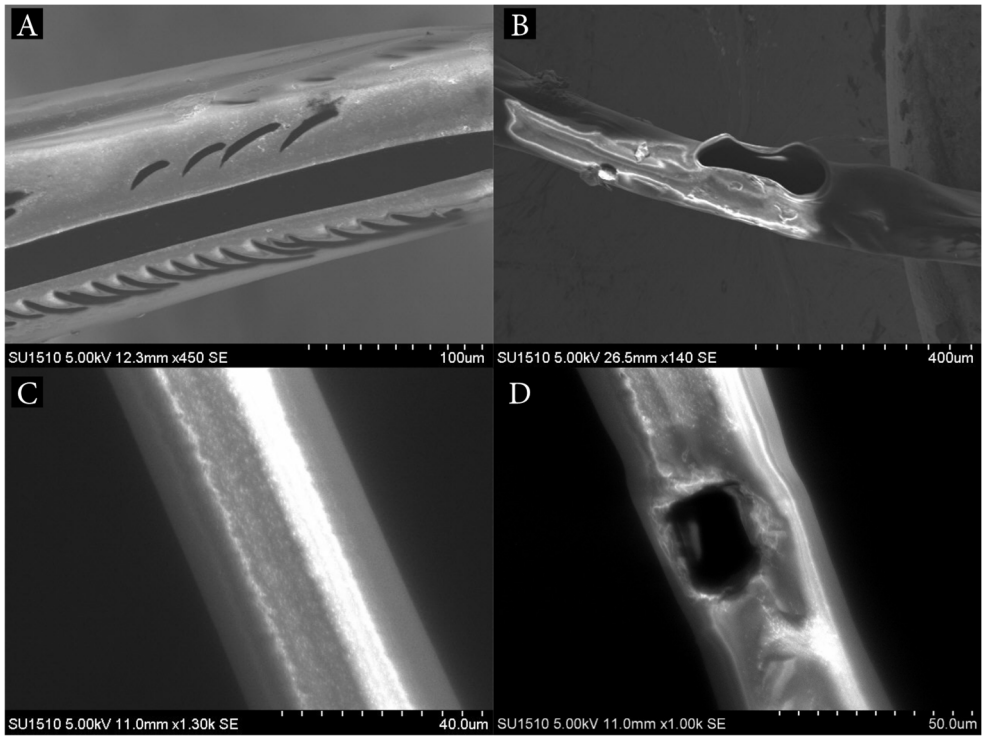

Figure 13. SEM images of tubular microelectrode after immersed in saline. (A) Shank and (B) hole opening of the tubular design with only gelatin as inner compartment. (C) Shank and (D) hole opening of the tubular design with an inner gelatin- and an outer glucose compartment. Modified from Paper III.

Design D was prepared by dip coating the gold wire in gelatin, followed by electrospinning of a glucose layer before insulating with Parylene-C. The design passed the initial integrity test in saline (Fig. 13C, D). It was hypothesised that the quickly dissolving glucose compartment created a space in which gelatin could swell which prevented rupture of the Parylene-C coating. The nanoparticles were embedded into the gelatin layer by absorption as in Paper II. As the wires were held by a frame, the whole frame would need to be immersed into the nanoparticle suspension. This would require a large volume (~30 mL) of suspended nanoparticles and a lot of material would be wasted by absorption into the gelatin coating on the frame´s edges. In order to minimize the consumption of the laboriously prepared nanoparticles, a new method was developed. The wires were instead dragged through a single drop (10 µL) of the nanoparticle suspension. After drying, the outer compartment of electro spun glucose was applied before insulating with Parylene-C.

Impedance measurement on the tubular electrode design D showed a quick decrease in impedance, stabilizing at 110 ± 20 kOhm (n = 5) at 1 kHz. It was concluded that the gelatin/nanoparticle coating did not compromise the electrodes functionality and that the design is suitable for electrophysiological recording.

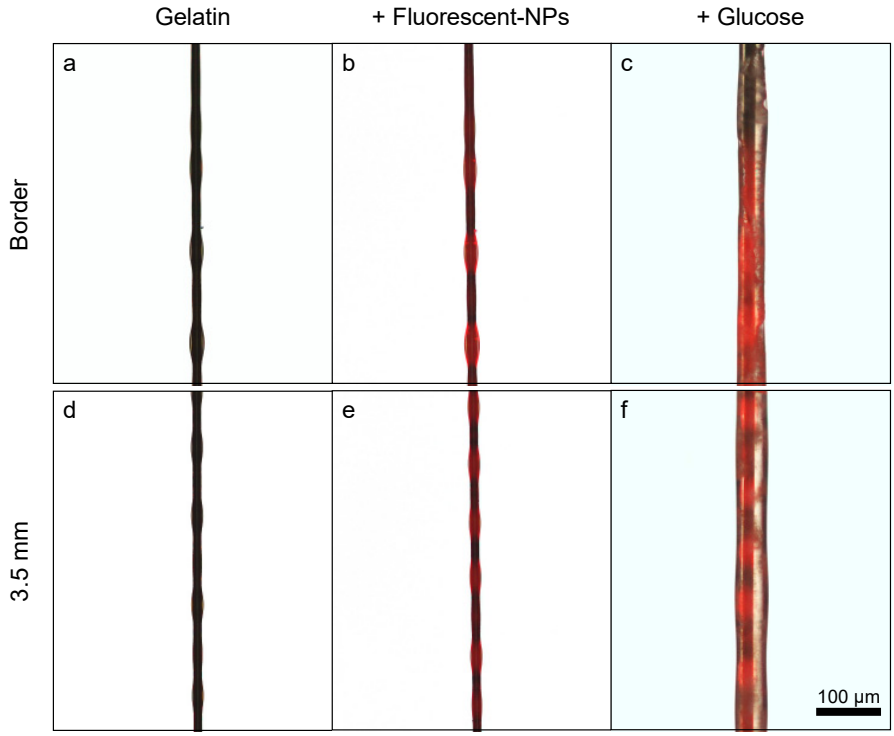

Figure 14. Brightfield and fluorescent images of a gold wire after coating with gelatin (a, d); absorption of fluorescent nanoparticles (NPs) (b, e); and electrospinning of glucose with one layer of Parylene-C (c, f). The images were taken at the gelatin dip border (a-c) and at 3.5 mm distance from the dip border (d-f). From Paper III.

Fluorescent and brightfield images of each applied layer (Fig. 14) shows that dip coating the gold wires resulted in a drop shaped layer of gelatin (Fig. 14a, d). The average dry drop diameter of was 22.2 ± 2.2 µm (mean ± standard deviation, n = 9) at the dipping boarder and 19.3 ± 1.7 µm at a 3.5 mm distance from the border. Figure 14(b, e) shows that the fluorescent nanoparticles were successfully absorbed into the gelatin coating without deforming the structure. Electrospinning of glucose and insulating with Parylene-C (Fig. 14c, f) resulted in a wavy outer structure. The gelatin/nanoparticle drops seemed to have increased in size, but this was however rather an optical effect from the rounded structure. It was concluded that the inner gelatin/nanoparticle layer had preserved its structure and that the added glucose had created an outer layer on top of the gelatin.

The *in vitro* release of the fluorescent nanoparticles was studied in agarose at 37 °C. The time series in Figure 15 shows that the fluorescent intensity becomes weaker in both directions from the tube opening as the inside of the tube gets wetted with time. It took approximately 1 hour for the tubes to be completely emptied. It was proposed that water from the surrounding enters the tube and quickly dissolves the glucose followed by gelatin swelling and release of nanoparticles inside the tube. As the tube continues to be filled with water, the gelatin coating dissolves and nanoparticles are released into the surrounding tissue.

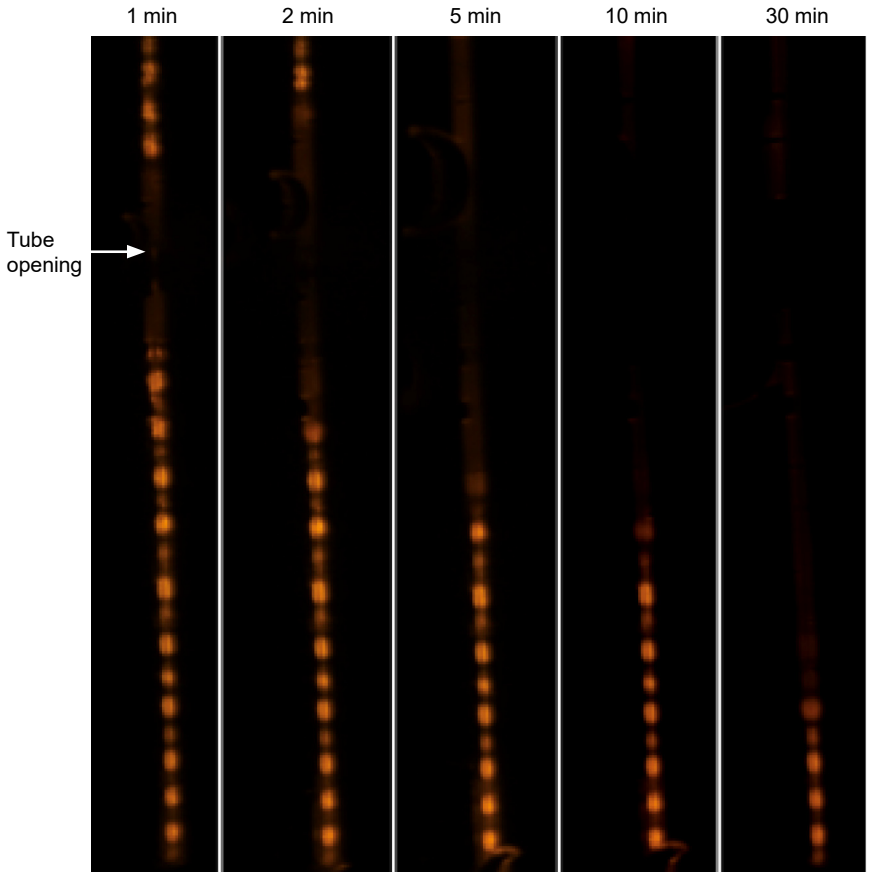

Figure 15. Image series of the *in vitro* release of fluorescently labeled nanoparticles from the tubular microelectrode in agarose**.** From Paper III

Discussion

The hypothesis in this thesis was that the biocompatibility of implanted neuroelectronic interfaces could be improved by a pharmacological approach. To this end, novel nanoparticle-based drug delivery systems were developed and evaluated *in vitro* and *in vivo*. In the first step, the drug Minocycline was encapsulated into biodegradable PLGA nanoparticles and thereby protected from degradation. This resulted in a sustained release for more than 30 days *in vitro*. In the next step, the drug-loaded nanoparticles were embedded in a fast-dissolving gelatin coating surrounding the implant thereby enabling local and sustained drug release at the target site. The developed drug delivery system was found to significantly attenuate the acute brain tissue responses around implanted micro-electrodes *in vivo*. In the last step, a novel nanoparticle-eluting compartmentalized microelectrode that transforms into a flexible tube once implanted was developed. Overall, the presented work brings a novel complementary strategy for improving biocompatibility of implanted neuro-electronic interfaces.

In vitro versus *in vivo*

Before evaluating the effects of the developed drug delivery systems in an animal study, the implants and nanoparticles were characterized *in vitro*. This was done in order to get a prediction on how the implants and drug delivery systems would behave *in vivo* and because some experiments are basically unfeasible to do *in vivo*. An *in vitro* study also enables comparison to work done by others. The drug content and entrapment efficiency of the nanoparticles developed in this work compares to what others have accomplished for Minocycline-loaded polymeric nanoparticles but the *in vitro* release time constitutes a substantial increase compared to what has been achieved until now [53, 54]. Comparison of *in vitro* drug-release profiles with others may however be misleading, as no standard testing procedures are used which may affect the release kinetics.

The *in vitro* test conditions in Paper I (in artificial cerebrospinal fluid at physiological pH and temperature) were chosen to mimic the prospective environment the nanoparticles were intended for. However, since the brain is an extremely complex environment it is difficult to cover all aspects.

The *in vitro* study in Paper II (in an agarose gel at room temperature) showed that the gelatin coating could withstand an implantation and also gave an idea of the nanoparticle release from the implant. The choice of doing the study at a lower temperature instead of at physiological temperature was done with regard to suggestions that the brain surface temperature is closer to room temperature during a craniotomy were the insulating layer of hair and skin has been removed [55]. No attempt was made to characterize the drug release in detail.

The *in vitro* study in Paper III was also done in an agarose gel, but in this study at a physiological temperature to mimic the brain environment around an implant after surgery. The study showed the nanoparticle release from the tubular electrode and that the implant could withstand implantation at an elevated temperature. Even though agarose gels are widely considered to be a viable *in vitro* model of the mechanical strength of the brain [42], it should be noted that diffusion of nanoparticles might differ substantially in the extracellular space compared to that in agarose [56, 57]. The "pore size" is bigger in agarose compared to in the extracellular space and the particles will therefore diffuse more freely in the model compared to in a live situation.

We also tried to examine the *in vivo* spreading of nanoparticles in a pilot study using gelatin coated implants with embedded fluorescent nanoparticles and looking for them 3 days after implantation. However, they were not to be found with either fluorescent or confocal microscopy. It was hypothesized that the amount of nanoparticles became too small in the tissue and the emitted fluorescence was below detection limits. Videos from the *in vitro* release studies of nanoparticles in agarose in paper II and III supported this notion. In paper II, it was clearly seen that the fluorescence became weaker the further away the particles came from the implant. In paper III, the particles could not even be seen after leaving the gelatin. Another possible "fate" *in vivo* is that the particles are phagocytosed by nearby microglia in which degradation of the particles might be faster compared to the *in vitro* milieu which would give a faster drug release kinetic.

As evident, there are a number of possibilities and aspects to consider when setting up *in vitro* studies. It comes to a point where further *in vitro* tests, evaluations and predictions will not give more insights for proving the hypothesis. A faster and perhaps more valid approach thereafter may be to study the effects *in vivo* instead. The overall purpose of this thesis was nevertheless to reduce brain tissue responses around implanted microelectrodes using a pharmacological strategy. In Paper II we showed that the developed nanoparticle drug delivery system indeed reduced the acute tissue reactions around implanted microelectrodes. The mechanisms behind the effects will however need further studies.

In vivo effects of Minocycline loaded nanoparticles

In Paper II it was shown that the Minocycline-loaded nanoparticles significantly reduced the microglial activation both after 3 and 7 days, and the astrocytic response after 7 days. These findings confirm and extend previously reported effects of Minocycline on microglia [58] and astrocytes [17]. It remains to be determined however, if the delayed effects on astrocytes found is a direct effect from Minocycline or a secondary effect from the decreased microglia activation at earlier time points.

It has been suggested that activated microglia polarize into two distinct functional phenotypes, pro-inflammatory (M1) and anti-inflammatory (M2). The M1-phenotype is associated with production of proinflammatory cytokines and chemokines that are involved in cytotoxicity and microbial killing. The M2-phenotype is associated with the expression of scavenger receptors and pro-angiogenic factors that promotes tissue repair and functional recovery [59, 60]. Minocycline's inhibitory effects on microglial activation has been readily studied and reports have also shown that Minocycline selectively inhibit microglial polarization into the M1 subgroup, thereby increasing the relative importance of the anti-inflammatory subgroup M2 [61, 62].

Evidence for that astrocytes also polarize into at least two types of phenotypes with different properties is emerging [63]. These are termed A1 and A2, one type being harmful and the other helpful for CNS recovery and repair. A1 astrocytes are neurotoxic and upregulate cascade genes shown to be destructive to synapses. A2 astrocytes upregulate neurotrophic factors that are shown be protective after injury. It has further been suggested that activated microglia induce A1 astrocytes [5].

The antibody (CD68) used to detect activated microglia in our study, stain both the M1 and the M2 microglial subgroups, but not unactivated microglia. The reduction of activated microglia is therefore likely related to a reduced number of M1 microglia given the established pharmacological mechanism of Minocycline. As a consequence, the number of activated astrocytes would also be reduced. Given the enormous complexity of the neuronal tissue, while possibly catching some of the mechanisms, this explanation of Minocycline´s effects is likely to be too simplistic. The situation is probably even more complex if other efforts involving changes in configuration and size of the electrodes [48, 64] are undertaken in order to reduce the acute tissue responses.

Acute response versus chronic response

Minimizing tissue responses from implanted neuroelectronic devices is necessary for obtaining high quality recordings that are stable for long periods of time. Studies have shown that the mechanical properties such as shape, flexibility and anchoring of the electrode are of great importance for lessening the chronic responses [1]. Moreover, the initial injury caused by the surgery and implantation itself has proven to be an important factor on the later chronic response [7]. Kumosa et al. [30] for example demonstrated that the astrocytic response in rat cortex can be seen for at least 6 weeks after a stab wound injury in the absence of a chronic implant. The study also showed that a gelatin coating could reduce this response significantly. The recently developed tubular microelectrode that is stiff enough to be implanted and then transforms into a flexible probe has proved to be highly biocompatible and essentially eliminates the loss of nearby neurons (Agorelius et al., 2020 unpublished). However, 6 weeks after implantation some remnants of astrocytic and microglial cells were observed around but also inside the tubes.

To further reduce the acute responses using a pharmaceutical approach as presented in this thesis brings in an additional factor. Paper II focused on responses that occurred during the first 7 days after implantation and both free floating implants and a gelatin coating were used in the study. As already mentioned, these two measures have proved to be important factors in reducing both acute and chronic responses [10, 50, 64]. The study demonstrated that Minocycline inhibited microglia activation and reduced the astrocytic response but showed no observable effects on neuronal survival. The lack of observable effects on neuronal survival might be due to that the neuroprotective effects of Minocycline are masked by improvements related to electrode design or that the effects of Minocycline on neuronal survival occur at later time points. The long-term effects of pharmaceutically reducing the acute responses needs to be evaluated further. One could speculate that the situation could be altered in the chronic phase. Minocycline and other anti-inflammatory drugs interfere after all with the CNS´s own protective and repairing mechanisms. Under normal circumstances, it might be harmful to disturb these balances. The brain may lose its own ability to for example fight off infections or remove dysfunctional neurons to preserve neuronal circuit functions. However, it is no longer a normal situation when an electrode is in the brain. Then it may be an idea to pharmaceutically modulate these mechanisms with the aim of maintaining that balance. Another speculation is that to much of M2 and lack of M1 microglia may lead to an excessive reconstruction of the tissue and result in an even thicker scar around the implant. These speculative scenarios would most likely also be dose dependent.

Concluding remarks and future perspective

The novel drug-delivery-systems for neural interfaces developed here provide highly localized effects in the tissue at the very electrode contact. By practically eliminating risks for systemic side effects this greatly improves the drug´s therapeutic efficacy as compared to systemic administration. Moreover, the tubular electrode construction developed in Paper III offers controlled release of biologically active compounds into the surrounding tissue directly outside the tubular orifice and recording site. This may be used to pharmacologically preserve the tissue of interest and inhibit migration of glial cells into the electrode to reduce the risk of clogging. While focusing on minocycline in this thesis, it is obvious that a similar approach may also be useful for other pharmaceutics and/or applications for which a highly localised effect is advantageous. The design also opens the possibilities to deliver and analyze highly localized effects of other drugs such as neurotrophic factors, with reduced confounding factors. From a drug development point of view, the hydrophobic ion pairing concept presented in Paper I may also be applicable to other water-soluble drugs and thereby enable use of preparation methods which are otherwise only suitable for lipophilic substances.

As a final note, it should be kept in mind that the brains immune system is truly an extraordinary complex system, developed through many years of evolution. Pharmaceutically altering this system should be done with great caution and with the aim of helping the brain maintain its ability to protect and repair itself.

Acknowledgments

I wish to express my sincere gratitude to:

Professor Jens Schouenborg, for introducing me into the field of neurophysiology and for stimulating scientific guidance.

Professor Ulf Nilsson, for stimulating collaboration, chemical guidance and support throughout this work.

Professor Nils Danielsen, for encouragement and support throughout this work.

Associate professor Cecilia Eriksson, for assistance with immunohistochemistry and support.

To all co-authors, former and present colleagues and office roommates, technical staff and administrative personal at the Centre for Analysis and Synthesis (CAS) and at Neuronano Research Center (NRC), for all help and good times at and after work.

To my family and friends, for your patience, love and support.

References

1. Lecomte, A., E. Descamps, and C. Bergaud, *A review on mechanical considerations for chronically-implanted neural probes.* Journal of Neural Engineering, 2018. **15**(3).
2. Polikov, V.S., P.A. Tresco, and W.M. Reichert, *Response of brain tissue to chronically implanted neural electrodes.* Journal of Neuroscience Methods, 2005. **148**(1): p. 1-18.
3. Riazi, K., M.A. Galic, J.B. Kuzmiski, W. Ho, K.A. Sharkey, and Q.J. Pittman, *Microglial activation and TNFα production mediate altered CNS excitability following peripheral inflammation.* Proceedings of the National Academy of Sciences, 2008. **105**(44): p. 17151.
4. Venero, J.L., M.A. Burguillos, P. Brundin, and B. Joseph, *The executioners sing a new song: killer caspases activate microglia.* Cell Death & Differentiation, 2011. **18**(11): p. 1679-1691.
5. Liddelow, S.A., K.A. Guttenplan, L.E. Clarke, F.C. Bennett, C.J. Bohlen, L. Schirmer, M.L. Bennett, A.E. Münch, W.-S. Chung, T.C. Peterson, D.K. Wilton, A. Frouin, B.A. Napier, N. Panicker, M. Kumar, M.S. Buckwalter, D.H. Rowitch, V.L. Dawson, T.M. Dawson, B. Stevens, and B.A. Barres, *Neurotoxic reactive astrocytes are induced by activated microglia.* Nature, 2017. **541**: p. 481.
6. Thelin, J., H. Jorntell, E. Psouni, M. Garwicz, J. Schouenborg, N. Danielsen, and C.E. Linsmeier, *Implant size and fixation mode strongly influence tissue reactions in the CNS.* PLoS One, 2011. **6**(1): p. e16267.
7. Wellman, S.M. and T.D.Y. Kozai, *Understanding the Inflammatory Tissue Reaction to Brain Implants to Improve Neurochemical Sensing Performance.* ACS Chemical Neuroscience, 2017. **8**(12): p. 2578-2582.
8. Lind, G., C.E. Linsmeier, and J. Schouenborg, *The density differences between tissue and neural probes is a key factor for glial scarring.* Scientific Reports., 2013. **3,** Article number: 2942.
9. O'Brien, D.P., T.R. Nichols, and M.G. Allen. Flexible microelectrode arrays with integrated insertion devices. Proceedings of the IEEE Micro Electro Mechanical Systems (MEMS), 2001. p. 216-219.
10. Lind, G., C.E. Linsmeier, J. Thelin, and J. Schouenborg, *Gelatine-embedded electrodes--a novel biocompatible vehicle allowing implantation of highly flexible microelectrodes.* Journal of Neural Engineering, 2010. **7**(4): p. 046005.
11. Farah, S., J.C. Doloff, P. Müller, A. Sadraei, H.J. Han, K. Olafson, K. Vyas, H.H. Tam, J. Hollister-Lock, P.S. Kowalski, M. Griffin, A. Meng, M. McAvoy, A.C. Graham, J. McGarrigle, J. Oberholzer, G.C. Weir, D.L. Greiner, R. Langer, and D.G.

Anderson, *Long-term implant fibrosis prevention in rodents and non-human primates using crystallized drug formulations.* Nature Materials, 2019. **18**(8): p. 892-904.

12. Arciola, C.R., D. Campoccia, and L. Montanaro, *Implant infections: adhesion, biofilm formation and immune evasion.* Nature Reviews Microbiology, 2018. **16**(7): p. 397-409.
13. Barza, M., R.B. Brown, C. Shanks, C. Gamble, and L. Weinstein, *Relation between lipophilicity and pharmacological behavior of minocycline, doxycycline, tetracycline, and oxytetracycline in dogs.* Antimicrobial Agents and Chemotherapy, 1975. **8**(6): p. 713-720.
14. Garrido-Mesa, N., A. Zarzuelo, and J. Gálvez, *Minocycline: far beyond an antibiotic.* British Journal of Pharmacology, 2013. **169**(2): p. 337-352.
15. Yrjänheikki, J., T. Tikka, R. Keinänen, G. Goldsteins, P.H. Chan, and J. Koistinaho, *A tetracycline derivative, minocycline, reduces inflammation and protects against focal cerebral ischemia with a wide therapeutic window.* Proceedings of the National Academy of Sciences of the United States of America, 1999. **96**(23): p. 13496-13500.
16. Noble, W., C.J. Garwood, and D.P. Hanger, *Minocycline as a potential therapeutic agent in neurodegenerative disorders characterised by protein misfolding.* Prion, 2009. **3**(2): p. 78-83.
17. Rennaker, R.L., J. Miller, H. Tang, and D.A. Wilson, *Minocycline increases quality and longevity of chronic neural recordings.* Journal of Neural Engineering, 2007. **4**(2): p. L1-L5.
18. Tikka, T., B.L. Fiebich, G. Goldsteins, R. Keinänen, and J. Koistinaho, *Minocycline, a Tetracycline Derivative, Is Neuroprotective against Excitotoxicity by Inhibiting Activation and Proliferation of Microglia.* The Journal of Neuroscience, 2001. **21**(8): p. 2580.
19. Fagan, S.C., D.J. Edwards, C.V. Borlongan, L. Xu, A. Arora, G. Feuerstein, and D.C. Hess, *Optimal delivery of minocycline to the brain: Implication for human studies of acute neuroprotection.* Experimental Neurology, 2004. **186**(2): p. 248-251.
20. Smith, K. and J.J. Leyden, *Safety of doxycycline and minocycline: A systematic review.* Clinical Therapeutics, 2005. **27**(9): p. 1329-1342.
21. Hussein, K., R. Bitterman, B. Shofty, M. Paul, and A. Neuberger, *Management of post-neurosurgical meningitis: narrative review.* Clinical Microbiology and Infection, 2017. **23**(9): p. 621-628.
22. Michel, V., D. Yoshiharu, H. Karl-Heinz, H. Michael, H. Philip, K. Przemyslaw, R. Marguerite, and S. François, *Terminology for biorelated polymers and applications (IUPAC Recommendations 2012).* Pure and Applied Chemistry, 2012. **84**(2): p. 377-410.
23. Garcia-Garcia, E., K. Andrieux, S. Gil, and P. Couvreur, *Colloidal carriers and blood–brain barrier (BBB) translocation: A way to deliver drugs to the brain?* International Journal of Pharmaceutics, 2005. **298**(2): p. 274-292.
24. Zhou, Y., Z. Peng, E.S. Seven, and R.M. Leblanc, *Crossing the blood-brain barrier with nanoparticles.* Journal of Controlled Release, 2018. **270**: p. 290-303.

25. Kumari, A., S.K. Yadav, and S.C. Yadav, *Biodegradable polymeric nanoparticles based drug delivery systems.* Colloids and Surfaces B: Biointerfaces, 2010. **75**(1): p. 1-18.
26. Kim, D.H. and D.C. Martin, *Sustained release of dexamethasone from hydrophilic matrices using PLGA nanoparticles for neural drug delivery.* Biomaterials, 2006. **27**(15): p. 3031-3037.
27. Kornev, V.A., E.A. Grebenik, A.B. Solovieva, R.I. Dmitriev, and P.S. Timashev, *Hydrogel-assisted neuroregeneration approaches towards brain injury therapy: A state-of-the-art review.* Computational and Structural Biotechnology Journal, 2018. **16**: p. 488-502.
28. Mercanzini, A., S.T. Reddy, D. Velluto, P. Colin, A. Maillard, J.C. Bensadoun, J.A. Hubbell, and P. Renaud, *Controlled release nanoparticle-embedded coatings reduce the tissue reaction to neuroprostheses.* Journal of Controlled Release, 2010. **145**(3): p. 196-202.
29. Jain, N., G.K. Jain, F.J. Ahmad, and R.K. Khar, *Validated stability-indicating densitometric thin-layer chromatography: Application to stress degradation studies of minocycline.* Analytica Chimica Acta, 2007. **599**(2): p. 302-309.
30. Kumosa, L.S., V. Zetterberg, and J. Schouenborg, *Gelatin promotes rapid restoration of the blood brain barrier after acute brain injury.* Acta Biomaterialia, 2018. **65**: p. 137-149.
31. Agorelius, J., F. Tsanakalis, A. Friberg, P.T. Thorbergsson, L.M. Pettersson, and J. Schouenborg, *An array of highly flexible electrodes with a tailored configuration locked by gelatin during implantation-initial evaluation in cortex cerebri of awake rats.* Frontiers in Neuroscience, 2015. **9**: p. 331.
32. Quintanar-Guerrero, D., E. Allémann, E. Doelker, and H. Fessi, *A mechanistic study of the formation of polymer nanoparticles by the emulsification-diffusion technique.* Colloid and Polymer Science, 1997. **275**(7): p. 640-647.
33. Fredenberg, S., M. Wahlgren, M. Reslow, and A. Axelsson, *The mechanisms of drug release in poly(lactic-co-glycolic acid)-based drug delivery systems - A review.* International Journal of Pharmaceutics, 2011. **415**(1-2): p. 34-52.
34. Zhong, Y. and R.V. Bellamkonda, *Biomaterials for the central nervous system.* Journal of the Royal Socity Interface, 2008. **5**(26): p. 957-75.
35. Kwon, H.Y., J.Y. Lee, S.W. Choi, Y. Jang, and J.H. Kim, *Preparation of PLGA nanoparticles containing estrogen by emulsification-diffusion method.* Colloids and Surfaces A: Physicochemical and Engineering Aspects, 2001. **182**(1-3): p. 123-130.
36. Ankola, D.D., E.W. Durbin, G.A. Buxton, J. Schäfer, U. Bakowsky, and M.N. Kumar, *Preparation, characterization and in silico modeling of biodegradable nanoparticles containing cyclosporine A and coenzyme Q10.* Nanotechnology, 2010. **21**(6): p. 065104.
37. Shahsavari, S., L. Rezaie Shirmard, M. Amini, and F. Abedin Dokoosh, *Application of Artificial Neural Networks in the Design and Optimization of a Nanoparticulate Fingolimod Delivery System Based on Biodegradable Poly(3-Hydroxybutyrate-Co-3-Hydroxyvalerate).* Journal of Pharmaceutical Sciences, 2017. **106**(1): p. 176-182.

38. McMurry, L.M., J.C. Cullinane, and S.B. Levy, *Transport of the lipophilic analog minocycline differs from that of tetracycline in susceptible and resistant Escherichia coli strains.* Antimicrobial Agents and Chemotherapy, 1982. **22**(5): p. 791-799.
39. Chow, K.T., L.W. Chan, and P.W.S. Heng, *Formulation of hydrophilic non-aqueous gel: Drug stability in different solvents and rheological behavior of gel matrices.* Pharmaceutical Research, 2008. **25**(1): p. 207-217.
40. Tosi, G., L. Bondioli, B. Ruozi, L. Badiali, G.M. Severini, S. Biffi, A. De Vita, B. Bortot, D. Dolcetta, F. Forni, and M.A. Vandelli, *NIR-labeled nanoparticles engineered for brain targeting: In vivo optical imaging application and fluorescent microscopy evidences.* Journal of Neural Transmission, 2011. **118**(1): p. 145-153.
41. Stetefeld, J., S.A. McKenna, and T.R. Patel, *Dynamic light scattering: a practical guide and applications in biomedical sciences.* Biophysical Reviews, 2016. **8**(4): p. 409-427.
42. Pomfret, R., G. Miranpuri, and K. Sillay, *The substitute brain and the potential of the gel model.* Annals of Neurosciences, 2013. **20**(3): p. 118-122.
43. Liu, Y., W. Wang, G. Acharya, Y.B. Shim, E.S. Choe, and C.H. Lee, *Advanced stent coating for drug delivery and in vivo biocompatibility.* Journal of Nanoparticle Research, 2013. **15**(10).
44. Lei, Y., H. Han, F. Yuan, A. Javeed, and Y. Zhao, *The brain interstitial system: Anatomy, modeling, in vivo measurement, and applications.* Progress in Neurobiology, 2017. **157**: p. 230-246.
45. Nicholson, C. and S. Hrabětová, *Brain Extracellular Space: The Final Frontier of Neuroscience.* Biophysical journal, 2017. **113**(10): p. 2133-2142.
46. Burda, J.E. and M.V. Sofroniew, *Reactive gliosis and the multicellular response to CNS damage and disease.* Neuron, 2014. **81**(2): p. 229-48.
47. Wang, Z., J. Nong, R.B. Shultz, Z. Zhang, T. Kim, V.J. Tom, R.K. Ponnappan, and Y. Zhong, *Local delivery of minocycline from metal ion-assisted self-assembled complexes promotes neuroprotection and functional recovery after spinal cord injury.* Biomaterials, 2017. **112**: p. 62-71.
48. Kumosa, L.S., V. Zetterberg, and J. Schouenborg, *Gelatin promotes rapid restoration of the blood brain barrier after acute brain injury.* Acta Biomaterialia, 2018. **65**: p. 137-149.
49. Köhler, P., A. Wolff, F. Ejserholm, L. Wallman, J. Schouenborg, and C.E. Linsmeier, *Influence of probe flexibility and gelatin embedding on neuronal density and glial responses to brain implants.* PLoS ONE, 2015. **10**(3).
50. Thelin, J., H. Jorntell, E. Psouni, M. Garwicz, J. Schouenborg, and N. Danielsen, *Implant size and fixation mode strongly influence tissue reactions in the CNS.* PLoS ONE, 2011. **6**.
51. De, S. and D.H. Robinson, *Particle size and temperature effect on the physical stability of PLGA nanospheres and microspheres containing bodipy.* The official journal of the Americal Association of Pharmaceutical Scientists, AAPS PharmSciTech, 2004. **5**(4).
52. Zbinovsky, V. and G.P. Chrekian, *Minocycline*, in *Analytical Profiles of Drug Substances*, F. Klaus, Editor. 1977, Academic Press. p. 323-339.

53. Kashi, T.S.J., S. Eskandarion, M. Esfandyari-Manesh, S.M.A. Marashi, N. Samadi, S.M. Fatemi, F. Atyabi, S. Eshraghi, and R. Dinarvand, *Improved drug loading and antibacterial activity of minocycline-loaded PLGA nanoparticles prepared by solid/oil/water ion pairing method.* International Journal of Nanomedicine, 2012. **7**: p. 221-234.
54. Yao, W., P. Xu, Z. Pang, J. Zhao, Z. Chai, X. Li, H. Li, M. Jiang, H. Cheng, B. Zhang, and N. Cheng, *Local delivery of minocycline-loaded PEG-PLA nanoparticles for the enhanced treatment of periodontitis in dogs.* International Journal of Nanomedicine, 2014. **9**: p. 3963-70.
55. Kalmbach, A.S. and J. Waters, *Brain surface temperature under a craniotomy.* Journal of Neurophysiology, 2012. **108**(11): p. 3138-3146.
56. Nicholson, C., K.C. Chen, S. Hrabětová, and L. Tao, *Diffusion of molecules in brain extracellular space: theory and experiment.* Progress in Brain Research, 2000. **125**: p. 129-54.
57. Pluen, A., P.A. Netti, R.K. Jain, and D.A. Berk, *Diffusion of macromolecules in agarose gels: comparison of linear and globular configurations.* Biophysical journal, 1999. **77**(1): p. 542-552.
58. McAllister Ii, J.P. and J.M. Miller, *Minocycline inhibits glial proliferation in the H-Tx rat model of congenital hydrocephalus.* Cerebrospinal Fluid Research, 2010. **7**.
59. Jang, E., S. Lee, J.H. Kim, J.H. Kim, J.W. Seo, W.H. Lee, K. Mori, K. Nakao, and K. Suk, *Secreted protein lipocalin-2 promotes microglial M1 polarization.* Journal of the Federation of American Societies for Experimental Biology, 2013. **27**(3): p. 1176-90.
60. Miron, V.E., A. Boyd, J.-W. Zhao, T.J. Yuen, J.M. Ruckh, J.L. Shadrach, P. van Wijngaarden, A.J. Wagers, A. Williams, R.J.M. Franklin, and C. ffrench-Constant, *M2 microglia and macrophages drive oligodendrocyte differentiation during CNS remyelination.* Nature Neuroscience, 2013. **16**(9): p. 1211-1218.
61. Kobayashi, K., S. Imagama, T. Ohgomori, K. Hirano, K. Uchimura, K. Sakamoto, A. Hirakawa, H. Takeuchi, A. Suzumura, N. Ishiguro, and K. Kadomatsu, *Minocycline selectively inhibits M1 polarization of microglia.* Cell Death & Disease, 2013. **4**(3): p. e525.
62. Papa, S., I. Caron, E. Erba, N. Panini, M. De Paola, A. Mariani, C. Colombo, R. Ferrari, D. Pozzer, E.R. Zanier, F. Pischiutta, J. Lucchetti, A. Bassi, G. Valentini, G. Simonutti, F. Rossi, D. Moscatelli, G. Forloni, and P. Veglianese, *Early modulation of pro-inflammatory microglia by minocycline loaded nanoparticles confers long lasting protection after spinal cord injury.* Biomaterials, 2016. **75**: p. 13-24.
63. Liddelow, S.A. and B.A. Barres, *Reactive Astrocytes: Production, Function, and Therapeutic Potential.* Immunity, 2017. **46**(6): p. 957-967.
64. Köhler, P., A. Wolff, F. Ejserholm, L. Wallman, J. Schouenborg, and C.E. Linsmeier, *Influence of probe flexibility and gelatin embedding on neuronal density and glial responses to brain implants.* PLoS One, 2015. **10**(3): p. e0119340.

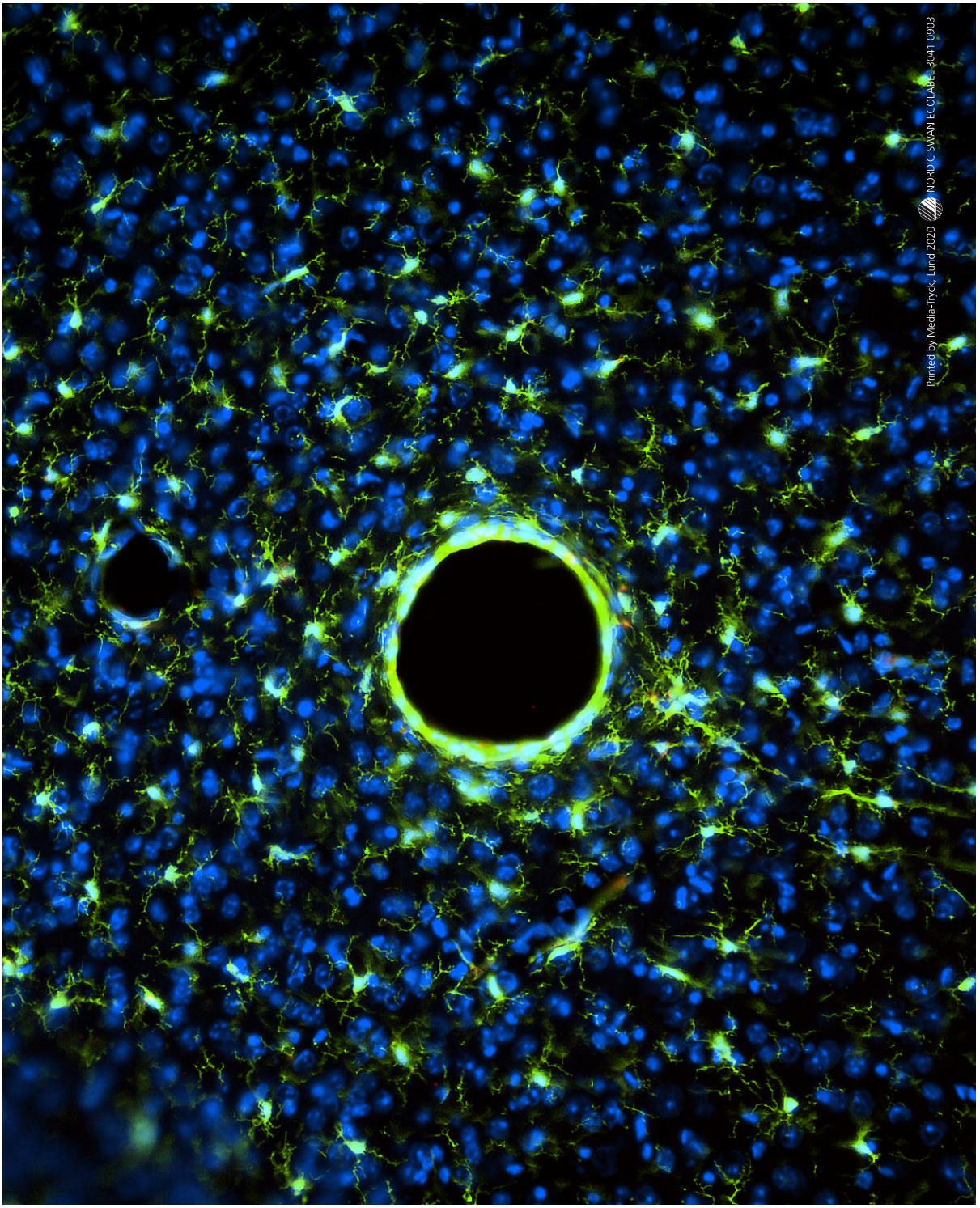

Printed by Media-Tryck, Lund 2020 NORDIC SWAN ECOLABEL 3041 0903

LUND UNIVERSITY

FACULTY OF MEDICINE

Department of Experimental Medical Science

Lund University, Faculty of Medicine
Doctoral Dissertation Series 2020:120
ISBN 978-91-7619-983-1
ISSN 1652-8220